



All Theses and Dissertations

2017-07-01

Effects of Curcumin and Ursolic Acid on the Mitochondrial Coupling Efficiency and Hydrogen Peroxide Emission of Intact Skeletal Myoblasts

Daniel J. Tueller
Brigham Young University

Follow this and additional works at: <https://scholarsarchive.byu.edu/etd>



Part of the [Nutrition Commons](#)

BYU ScholarsArchive Citation

Tueller, Daniel J., "Effects of Curcumin and Ursolic Acid on the Mitochondrial Coupling Efficiency and Hydrogen Peroxide Emission of Intact Skeletal Myoblasts" (2017). *All Theses and Dissertations*. 6911.
<https://scholarsarchive.byu.edu/etd/6911>

This Thesis is brought to you for free and open access by BYU ScholarsArchive. It has been accepted for inclusion in All Theses and Dissertations by an authorized administrator of BYU ScholarsArchive. For more information, please contact scholarsarchive@byu.edu, ellen_amatangelo@byu.edu.

Effects of Curcumin and Ursolic Acid on the Mitochondrial Coupling Efficiency
and Hydrogen Peroxide Emission of Intact Skeletal Myoblasts

Daniel J. Tueller

A thesis submitted to the faculty of
Brigham Young University
in partial fulfillment of the requirements for the degree of
Master of Science

Chad R. Hancock, Chair
Merrill J. Christensen
Jeffery S. Tessem

Department of Nutrition, Dietetics, and Food Science
Brigham Young University

Copyright © 2017 Daniel J. Tueller

All Rights Reserved

ABSTRACT

Effects of Curcumin and Ursolic Acid on the Mitochondrial Coupling Efficiency and Hydrogen Peroxide Emission of Intact Skeletal Myoblasts

Daniel J. Tueller

Department of Nutrition, Dietetics, and Food Science, BYU
Master of Science

Curcumin is a natural compound that improves blood glucose management. While some evidence from isolated mitochondria indicates that curcumin uncouples electron transport from oxidative phosphorylation, the effects of curcumin on mitochondrial respiration and hydrogen peroxide emission in intact skeletal muscle cells are not known. By assessing rates of oxygen consumption, we demonstrated for the first time that curcumin (40 μ M) reduced the mitochondrial coupling efficiency (percentage of oxygen consumption that supports ATP synthesis) of intact skeletal muscle cells. A 30-minute incubation with curcumin decreased mitochondrial coupling efficiency by $17.0 \pm 0.4\%$ relative to vehicle ($p < 0.008$). Curcumin also decreased the rate of hydrogen peroxide emission by $43 \pm 13\%$ compared to vehicle ($p < 0.05$). Analysis of cell respiration in the presence of curcumin revealed a $40 \pm 4\%$ increase in the rate of oxygen consumption upon curcumin administration ($p < 0.05$ compared to vehicle). In additional experiments, no difference in mitochondrial coupling efficiency was observed between vehicle- and curcumin-pretreated cells after permeabilization of cell membranes ($p > 0.7$). The possibility of synergistic effects between curcumin and ursolic acid, another natural compound that improves blood glucose management, was also examined. Interestingly, ursolic acid (0.12 μ M) increased mitochondrial coupling efficiency by $4.1 \pm 1.1\%$ relative to vehicle ($p < 0.008$) and attenuated the effect of curcumin when the two compounds were used in combination (decreased mitochondrial coupling efficiency by $8.0 \pm 0.9\%$ compared to vehicle, $p < 0.008$). These results provide evidence for lower mitochondrial coupling efficiency and hydrogen peroxide emission as possible contributors to the increased glucose uptake and insulin sensitivity of subjects after treatment with curcumin but not ursolic acid. Unless cells are assessed in the intact condition, changes to mitochondrial coupling efficiency after curcumin treatment may go unnoticed.

Keywords: curcumin, mitochondria, skeletal muscle, ursolic acid

ACKNOWLEDGEMENTS

I would like to thank Dr. Hancock for allowing me to work under his direction in this graduate program. I am grateful for the tremendous opportunity he afforded me to design and implement my project. His counsel throughout the way was invaluable for the success of this study and for my personal growth as well. I also appreciate the guidance of my other committee members, Dr. Christensen and Dr. Tessem, who warmly lent me their expertise in addition to advice for my future.

Many of the experiments included in this project were performed by Jackson Harley. I am thankful for both his technical assistance and his enthusiasm that helped to push the project forward. I am also grateful for the support of other members within Dr. Hancock's lab group: Amy Mackay, Jake Anderson, Devin Munk, Andrew Jefferson, Boden Christianson, and Andrew Damron, who all helped to make this study a great experience.

TABLE OF CONTENTS

TITLE PAGE	i
ABSTRACT.....	ii
ACKNOWLEDGEMENTS	iii
TABLE OF CONTENTS.....	iv
LIST OF TABLES	vi
LIST OF FIGURES	vii
INTRODUCTION	1
Hyperglycemia and insulin resistance	1
Nutrient overload and insulin signaling.....	1
Curcumin and ursolic acid	3
Study objectives	6
METHODS	7
Cell culture.....	7
Intact cell respiration.....	8
Permeabilized cell respiration.....	12
Hydrogen peroxide emission	16
Treatments.....	17
Coupling efficiency.....	19
Statistics	20

RESULTS	21
Mitochondrial coupling efficiency.....	21
Hydrogen peroxide emission	25
Experiments without pyruvate and phenol red	28
Immediate effect of curcumin treatment on rate of oxygen consumption	32
Permeabilization of cells after 30-minute pretreatment.....	35
DISCUSSION	37
Objectives	37
Curcumin and glucose uptake.....	38
Curcumin and insulin sensitivity	39
Ursolic acid.....	43
Synergism	45
Permeabilization	46
CONCLUSION.....	52
REFERENCES	53

LIST OF TABLES

Table 1. Mitochondrial coupling efficiency of intact C2C12 myoblasts after pretreatment.	22
Table 2. Rates of oxygen consumption of intact myoblasts after 30-minute pretreatment.	23
Table 3. Rates of hydrogen peroxide emission from intact C2C12 myoblasts.....	26
Table 4. Mitochondrial coupling efficiencies of intact and permeabilized C2C12 myoblasts.	29
Table 5. Rates of oxygen consumption of intact myoblasts in media without pyruvate.	30
Table 6. Rates of hydrogen peroxide emission from myoblasts in media without pyruvate.....	31
Table 7. Mitochondrial respiration of intact C2C12 myoblasts in the presence of treatment.	34
Table 8. Rates of oxygen consumption of pretreated myoblasts after permeabilization.	36

LIST OF FIGURES

Figure 1. Annotated display from an intact-cell respiration experiment.	11
Figure 2. Annotated display from a permeabilized-cell respiration experiment.	15
Figure 3. Mitochondrial coupling efficiency of intact C2C12 myoblasts.	24
Figure 4. Rate of hydrogen peroxide emission from intact C2C12 myoblasts.	27
Figure 5. Annotated results of two simultaneous experiments with intact C2C12 myoblasts.	33

INTRODUCTION

Hyperglycemia and insulin resistance

Impaired blood-glucose control is a widely accepted contributor to the development of chronic disease (Centers for Disease Control and Prevention, 2014). The regulation of blood glucose is largely mediated by the hormone insulin, which signals the uptake of glucose from the blood into insulin-sensitive tissues by promoting the translocation of the glucose transporter GLUT4 from the cell cytosol to the plasma membrane (Di Meo, Iossa, and Venditti, 2017). Insulin resistance, or the decreased capacity of cells to respond to insulin, impairs blood-glucose management by necessitating a larger insulin stimulus to maintain a normal concentration of blood glucose. Because skeletal muscle accounts for the vast majority of glucose uptake after a meal (Baron et al., 1988; DeFronzo and Tripathy, 2009), treatments that promote insulin sensitivity in skeletal muscle cells have tremendous potential to alleviate hyperglycemia and the progression of associated pathogenic conditions such as type 2 diabetes, obesity, and atherosclerosis (Affourtit, 2016).

Nutrient overload and insulin signaling

The shift in cellular redox environment that results from nutrient overload has been hypothesized as a contributor to insulin resistance (Fisher-Wellman and Neuffer, 2012). According to this hypothesis, excessive fuel supply in the absence of matching demand leads to increased mitochondrial production of reactive oxygen species. The amount of reactive oxygen species increases during such fuel imbalance because the mitochondrial electron transport system is presented with an overabundance of electrons, which come from carbohydrate, lipid, and protein oxidation. Electrons are passed between protein complexes along the electron transport system in a series of oxidation-reduction reactions until ultimately uniting with oxygen and

hydrogen to form water (Mailloux, 2015). This last step, where oxygen acts as the final electron acceptor in the electron transport system, is the main reaction responsible for the use or consumption of oxygen (respiration) in our cells and is a reason why oxygen is so vital for life.

A molecule is said to undergo oxidation when it gives up its electrons, and a molecule is reduced when it receives electrons. If the amount of electron carriers (also called reducing equivalents due to their propensity to reduce, or transfer electrons to, other compounds) is high, such as after excessive energy intake, then more electrons will be delivered from these carriers to the electron transport system. This means that a greater percentage of electron-transport-system complexes will exist in their reduced state and that less will exist in their oxidized state (Fisher-Wellman and Neuffer, 2012). With less complexes available to accept electrons within the transport system, there is an increased likelihood that electrons will pass out of the transport system and react with oxygen prematurely to generate reactive oxygen species. The first radical that forms from the union of molecular oxygen with a single electron is superoxide, which is quickly converted by superoxide dismutase enzymes into hydrogen peroxide (Brand, 2016). Hydrogen peroxide can then be reduced to water by the glutathione or thioredoxin/peroxiredoxin antioxidant enzyme systems. Through this neutralization process, antioxidant enzymes protect cell structures from damage than could be induced by reactive oxygen species. A consequence is that these protective enzymes are oxidized during the act of hydrogen-peroxide neutralization, and the intracellular environment of the cell will then shift toward a more general state of oxidation (Schafer and Buettner, 2001; Fisher-Wellman and Neuffer, 2012). Such a shift in redox environment leads to increased activity of certain enzymes such as c-Jun amino-terminal kinases (Aguirre et al., 2000; Rindler et al., 2013), which phosphorylate serine and threonine residues on insulin receptor substrates 1 and 2 (IRS1 and IRS2). Proper insulin signaling requires the

phosphorylation of tyrosine residues on IRS1 and IRS2 in order to allow docking of downstream effector molecules, but this docking cannot occur when serine and threonine residues on these proteins are phosphorylated instead of tyrosine (Di Meo, Iossa, and Venditti, 2017). This altered phosphorylation pattern therefore disrupts the propagation of the insulin signal and ultimately impairs the translocation of GLUT4 proteins from the cytosol to the membrane of the cell (Carnagarin, Dharmarajan, and Dass, 2015).

Based on the effect of cellular redox environment on insulin signal proteins, effective insulin signaling may be restored through means that prevent a buildup of reducing equivalents in mitochondria (Muoio and Neuffer, 2012). This concept has been demonstrated in experiments where the administration of a beta-oxidation inhibitor (which prevented the transport of fatty acids into mitochondria and thus limited the production of reducing equivalents from fatty-acid oxidation) improved the insulin sensitivity of mice (Finck et al., 2005). Consistent with this hypothesis, lifestyle changes that promote negative energy balance through either diet (lower energy intake) or exercise (increased energy expenditure) both contribute to improved insulin sensitivity and blood glucose management (Dube et al., 2011).

Curcumin and ursolic acid

Clinical studies have demonstrated that curcumin, a compound isolated from the common spice, turmeric, improves insulin sensitivity and glycemic control in humans (Chuengsmarn et al., 2012; Na et al., 2013; Chuengsmarn et al., 2014). Although a host of potential molecular targets and actions of curcumin have been identified (Ghosh, Banerjee, and Sil, 2015; Jiménez-Osorio, Monroy, and Alavez, 2016), curcumin's effect on mitochondrial respiration remains unclear. Some interesting findings involving isolated mitochondria provided evidence that curcumin may uncouple the electron transport system from ATP production (Lim, Lim, and

Wong, 2009; Martineau, 2012). Normally, electron transport and oxidative phosphorylation are tightly coupled, meaning that most of the potential energy generated from electron transport is used to drive ATP synthesis. These two processes (electron transport and oxidative phosphorylation) are linked by a gradient of protons that are pumped out of the mitochondrial matrix during electron transport and then flow back into the matrix through the ATP synthase enzyme. If the electron transport system and ATP production become uncoupled, more substrate would be required to maintain an optimal rate of ATP synthesis (Klip et al., 2009). This concept has been illustrated in mice that were genetically engineered to exhibit greater uncoupling between electron transport and oxidative phosphorylation; these mice displayed greater fuel uptake and turnover than their wildtype counterparts (Clapham et al., 2000). A similar coupling inefficiency could contribute to the increased glucose uptake, independent from any changes to insulin signaling, that was observed in skeletal muscle cells after curcumin treatment (Kang and Kim, 2010; Kim et al., 2010, Na et al., 2011) since more fuel may be needed during reduced mitochondrial coupling in order to maintain ATP production. However, the effect of curcumin on mitochondrial coupling efficiency in skeletal muscle cells has not been assessed.

Lower mitochondrial coupling efficiency may also contribute to curcumin's positive effect on insulin sensitivity. If coupling between the electron transport system and oxidative phosphorylation is decreased, then the ATP yield from a given amount of fuel would also be reduced. More fuel would therefore be required to maintain an optimal ATP concentration within the cell. The likelihood of an accumulation of reducing equivalents in mitochondria would decrease, and less reactive oxygen species would be generated. This principle has also been demonstrated in mice where the intentional uncoupling of electron transport from oxidative phosphorylation in skeletal muscle led to decreased hydrogen peroxide production (Anderson,

Yamazaki, and Neuffer, 2007) and improved insulin sensitivity (Li et al., 2000; Bernal-Mizrachi et al., 2002; Han et al., 2004; Katterle et al., 2008; Neschen et al., 2008; Keipert, Voigt, and Klaus, 2011; Adjeitey et al., 2013; Keipert et al., 2013). The administration of therapeutic compounds that reduce mitochondrial coupling similarly improved the insulin sensitivity of mice (Perry et al., 2013; Perry et al., 2015). As curcumin's effects on the mitochondrial coupling efficiency and hydrogen peroxide emission of skeletal muscle cells have not yet been assessed, the identification of any effects if present would increase our understanding of why curcumin treatment may improve blood-glucose management and insulin sensitivity.

Unfortunately, poor absorption and rapid clearance from the body are major limitations to curcumin's therapeutic potential (Salem, Rohani, and Gillies, 2014; Mirzaei et al., 2017). The bioavailability of curcumin after oral intake has been estimated to be around 1% (Yang et al., 2007). While efforts have been undertaken to improve curcumin delivery into tissues (Prasad, Tyagi, and Aggarwal, 2014; Liu et al., 2016), another way to circumvent curcumin's poor bioavailability may be to administer curcumin with a synergistically acting compound. Such a combination could decrease the concentration of curcumin that is required to yield beneficial effects. Ursolic acid, found in a number of fruits, has improved the insulin sensitivity and blood-glucose management of mice (Jang et al., 2009; Kunkel et al., 2012; Li et al., 2014; Jia et al., 2015). Similar to curcumin, ursolic acid also stimulated oxygen consumption in the absence of ATP synthesis in isolated mitochondria (Liobikas et al., 2011). This change in mitochondrial respiration was also associated with decreased hydrogen peroxide production. The effect of ursolic acid on mitochondrial coupling efficiency and hydrogen peroxide emission has not been explored in intact skeletal muscle cells. If such effects are induced by both ursolic acid and curcumin in skeletal muscle cells, then a combination with these two treatments could allow a

lower curcumin dose to be used in therapies to achieve benefits on blood-glucose management. This possibility is even more tantalizing in light of recent evidence that curcumin and ursolic acid acted synergistically to decrease the size of prostate tumors in mice (Lodi et al., 2017). Reduced mitochondrial coupling has previously been identified as a potential contributor to the success of some chemotherapeutic compounds (Marín-Prida et al., 2017). However, the interaction between curcumin and ursolic acid on mitochondrial coupling efficiency or hydrogen peroxide emission has not been assessed in any model. If synergism were present between curcumin and ursolic acid on these aspects of mitochondrial function within intact skeletal muscle cells, a combined treatment with these two compounds would have great therapeutic potential to improve blood-glucose control and insulin sensitivity.

Study objectives

The main objective of this study was to determine if curcumin decreases the mitochondrial coupling efficiency and hydrogen peroxide emission of intact skeletal muscle cells. The presence of such effects in intact skeletal muscle cells would provide new insight to how curcumin may have improved the blood-glucose control and insulin sensitivity of subjects in past experiments. An additional objective was to determine if curcumin and ursolic acid act synergistically to modulate the mitochondrial coupling efficiency and hydrogen peroxide emission of intact skeletal muscle cells. Part of this objective involved the determination of ursolic acid's individual effects on the mitochondrial coupling efficiency and hydrogen peroxide emission of intact skeletal muscle cells, as these effects are also not known. If curcumin and ursolic acid act synergistically to decrease the mitochondrial coupling efficiency and hydrogen peroxide emission of intact skeletal muscle cells, then a lower curcumin dose could theoretically be used to improve insulin sensitivity and blood-glucose management.

METHODS

Cell culture

C2C12 myoblasts (ATCC® CRL-1772™), an immortalized skeletal muscle cell line originally isolated from the thigh of adult mice (Yaffe and Saxel, 1977), were chosen as an experimental model. Since skeletal muscle is responsible for the vast majority of insulin-mediated glucose uptake (Baron et al., 1988), treatments that increase insulin sensitivity in skeletal muscle cells would have tremendous potential to improve blood glucose homeostasis. This model was chosen over other skeletal muscle cell lines because C2C12 cells are widely used and have been employed in previous studies involving curcumin and ursolic acid (Kang and Kim, 2010; Deng et al., 2012, Figueiredo and Nader, 2012; Martineau, 2012). The cells originate in the myoblast stage where they rapidly divide. Upon becoming confluent, the cells differentiate into myotubes; they fuse together, become multinucleated and elongated, and spontaneously contract. While most previous experiments that used C2C12 cells with curcumin and ursolic acid were performed using myotubes, the present study was conducted with cells in the myoblast stage. This decision was the result of extensive preliminary experiments in which the viability of myotubes could not be ensured over the duration of respiration experiments. Respiration experiments using samples of soleus and gastrocnemius tissue from rats and mice were also attempted unsuccessfully, possibly due to compromised plasma membrane integrity in these models (Pesta and Gnaiger, 2012). A more detailed explanation regarding the importance and challenges of preserving membrane integrity during respiration experiments is offered in the discussion section of the present paper. Although our experiments with myotubes and muscle fiber bundles were not successful, C2C12 myoblasts still provided a model of intact skeletal muscle cells in which our objectives could be carried out.

The protocol employed for cell culture was adapted from previously described methods (Fisher-Wellman et al., 2014; Kwak et al., 2012). In preparation for experiments, myoblasts were seeded at approximately 1×10^4 cells/cm² in 6-well plates. Cells were cultured in growth media that consisted of Dulbecco's Modified Eagle's Medium (SIGMA D6429), 10% fetal bovine serum, and 1% antibiotic antimycotic solution (10,000 U penicillin, 10 mg streptomycin, and 25 µg amphotericin B per mL) in a 5% CO₂ environment at 37 °C. Differentiation into myotubes was enhanced after cells reached 100% confluency by replacing growth media with differentiation media, which contained the same formulation as growth media except for a substitution of adult horse serum in place of fetal bovine serum. Myoblasts (after reaching 90% confluency) and myotubes (after 3 days on differentiation media) to be used for experiments were rinsed twice with Hank's Balanced Salt Solution (lacking calcium and magnesium) and then rinsed once with 0.05% trypsin EDTA. Cells were then incubated at 37 °C until detached from plates and were then suspended in fresh culture media.

Intact cell respiration

Measurement of cell respiration was performed using a Clark-type oxygen-electrode respirometer/fluorometer (Oxygraph-2k, OROBOROS INSTRUMENTS). This instrument functions by detecting the electrical current, or movement of electrons, associated with the reduction of oxygen in solution within an enclosed chamber (referred to hereafter as the respiratory chamber). By calibrating the instrument under conditions of both atmospheric and zero oxygen concentrations, a slope can be generated and used to convert the detected electric current in the respiratory chamber to measurements of oxygen concentration over the course of an experiment (Clark and Sachs, 1968; LeFevre, 1969).

The methods used for assessment of cell respiration in the present study were modified from previously established protocols (Pesta and Gnaiger, 2012). After the addition of cell suspension to the respiratory chamber, cells were spun for 10 minutes at 25 °C and 750 RPM in cell culture media and then sampled for measurement of cell count and viability using a hemocytometer and the Trypan Blue exclusion method. Trypan Blue is a blue-colored compound that cannot cross an intact cell membrane. The presence of blue-colored cells after treatment with Trypan Blue thus reveals cellular damage or death. Only experiments in which samples were greater than 95% viable, as assessed using this method, were included in the final data analysis. Viability was calculated as the number of viable cells divided by the total number of viable and damaged cells. On average, approximately 3.5 million viable cells (1.75 million/mL) were assessed during each experiment. This was the typical yield from three wells of a 6-well plate and was used in order to obtain a volume-specific rate of oxygen consumption of around 20 pmol/s*mL or higher during routine respiration (Pesta and Gnaiger, 2012).

After counting the cells and assessing their viability, the respiratory chamber was closed, and the rate of oxygen consumption was given time to stabilize. This steady state (Figure 1), where respiration was supported by the nutrients in cell culture media, principally glucose (22.2 mM) and pyruvate (0.89 mM), was characterized as routine respiration (R). The rate of oxygen consumption during this period was also supported by endogenous ADP within cells and was therefore an indicator of oxidative phosphorylation-supported respiration as well. Oligomycin (2.5 μ M), which inhibits oxidative phosphorylation by blocking ATP synthase, was then added to the respiratory chamber. The rate of oxygen consumption was then allowed to stabilize again. Since the proton gradient generated by the electron transport system cannot not be dissipated through ATP synthase in the presence of oligomycin, mitochondrial oxygen consumption during

this condition was only possible via proton transport by other means across the inner mitochondrial membrane into the matrix (Divakaruni and Brand, 2011). This transport, referred to as proton leak, may occur through passive diffusion or through conductance mediated by other proteins in the mitochondrial membrane (Jastroch et al., 2010; Brand and Nicholls, 2011). Without such leak, the pressure of protons outside of the matrix would become so great as to prevent any additional passage of electrons through the electron transport system. This state was therefore characterized as leak-supported respiration (L). Lastly, antimycin A (2.5 μM), which inhibits electron transport through complex III (the convergence point for electrons from complexes I and II), was added to the respiratory chamber to halt all oxygen consumption associated with the electron transport system. The residual rate of oxygen consumption (ROX) that remained after antimycin A administration was subtracted from the raw measurements taken during the previous respiratory states as part of our data analysis. Accounting for ROX allowed data to be corrected for any background oxygen consumption from sources extraneous to the electron transport system.

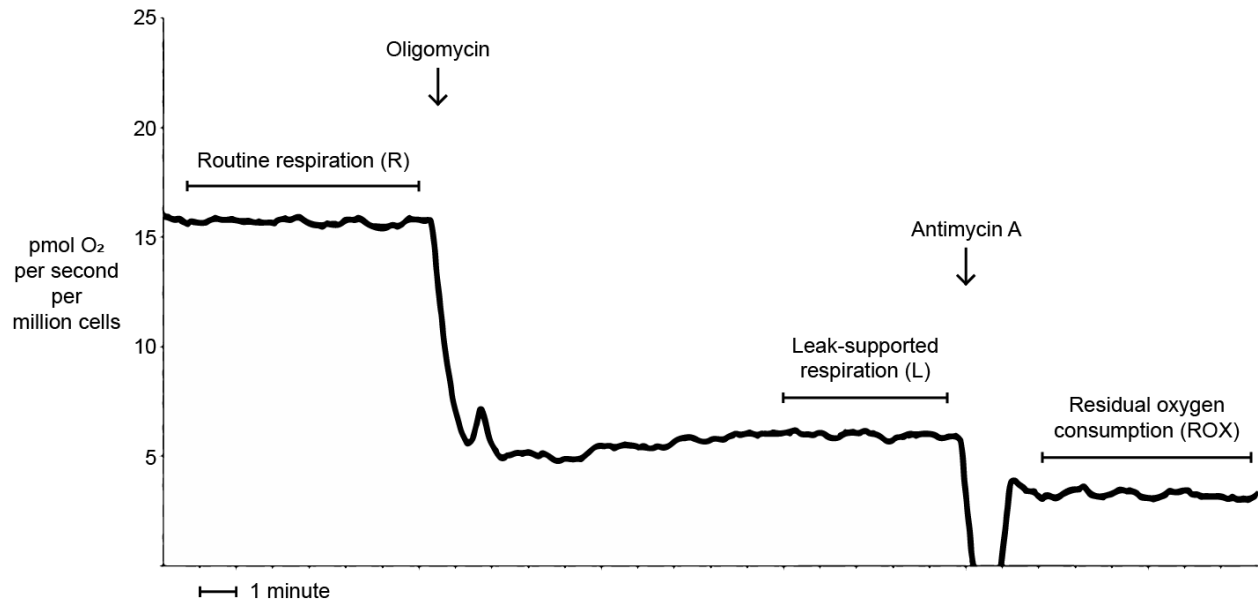


Figure 1. Annotated display from an intact-cell respiration experiment.

^R Supported by glucose and pyruvate in cell culture media as well as by endogenous ADP within cells.

^L Maintained by glucose, pyruvate, and proton leak after inhibition of ATP synthase.

^{ROX} Residual oxygen consumption after inhibition of complex III.

During experiments with intact and permeabilized myoblasts, the oxygen concentration in the respiratory chamber was maintained at approximately 100-200 μM . This was achieved by initiating experiments at an oxygen level near air saturation and then completing the assessment of respiration before oxygen levels dropped below 100 μM . Although these concentrations were higher than physiological intracellular oxygen levels (Gnaiger et al., 1998; Gnaiger, Méndez, and Hand, 2000; Gnaiger and Kuznetsov, 2002), the chosen oxygen concentration range was used in order to prevent the rate of oxygen diffusion across cells from limiting respiratory activity. Such a limitation may lead to suboptimal respiration if oxygen diffusion from the extracellular environment to mitochondria occurs at a slower rate than oxygen consumption during respiration (Scandurra and Gnaiger, 2010). Experiments with permeabilized muscle tissue, for example, must be performed using oxygen concentrations above air saturation (typically 250-500 μM) in order to prevent oxygen diffusion from limiting respiration (Pesta and Gnaiger, 2010). These concentrations are necessary when using muscle fiber bundles because of the greater diffusion distance (over 150 μm) that oxygen must travel in order to reach the fiber core (Gnaiger, 2003). Small cells, on the other hand, with diffusion distances of only 5-10 μm , can be assessed using oxygen levels as low as 20 μM without limiting respiration (Pesta and Gnaiger, 2010). Preliminary experiments in the present study support these past findings in that we observed no limitation to the rate of oxygen consumption of intact C2C12 myoblasts with oxygen concentrations as low as 30 μM .

Permeabilized cell respiration

A separate protocol was used to assess respiration in permeabilized cells. Once harvested, cells were centrifuged at 86 RCF for 5 minutes. This speed was the lowest possible on available instrumentation and was selected to minimize the risk of mitochondrial damage after the harvest

process. Growth media was then removed, and cells were suspended in respiration buffer (MiR05) containing 110 mM sucrose, 60 mM potassium lactobionate, 3 mM magnesium chloride, 20 mM taurine, 10 mM potassium phosphate, 0.5 mM EGTA, 20 mM HEPES, and 1 g/L BSA. Although cell culture media is ideal for measurement of respiration with intact cells (due to provision of the same substrate and ion concentrations that support optimal cell health), MiR05 was used for permeabilized cells because the calcium concentration in cell culture media is damaging to mitochondria (Gnaiger et al., 2000; Lemasters et al., 2009).

After transferring the cell suspension to the respiratory chamber, the chamber was closed, and glutamate (10 mM), malate (2 mM), and digitonin (4.1 μ M) were added to the chamber. The oxidation of malate to oxaloacetate during the tricarboxylic acid (TCA) cycle results in the transfer of electrons to NADH, which delivers electrons to complex I of the electron transport system (Gnaiger, 2009). Provision of malate alone leads to oxaloacetate accumulation and inhibition of TCA cycle activity, so glutamate is added first to maintain TCA cycle function. Glutamate reacts with oxaloacetate in a transaminase reaction to form α -ketoglutarate, another TCA cycle intermediate, and this reaction yields NADH in as well. Glutamate and malate were added immediately prior to digitonin in order to support respiration while digitonin took effect. Digitonin interacts with cholesterol in cell membranes to form complexes that partially open the membrane (Salabei, Gibb, and Hill, 2014). As a result of these openings, any endogenous substrates within cells were washed out and were present in the respiratory chamber at much lower concentrations than what the mitochondria would experience in an intact cell. Permeabilization in this manner is typically performed in order to provide researchers with greater control over the substrate environment. Since cholesterol is abundant in plasma membranes but not in other organelles, low concentrations of digitonin will not damage

mitochondria. Succinate (10 mM) and octanoylcarnitine (0.2 mM) were then added to additionally stimulate respiration. Succinate is oxidized as part of the TCA cycle by succinate dehydrogenase, which is the main polypeptide of complex II. Succinate thus supplies electrons directly to the electron transport system through that complex. Through β -oxidation, octanoylcarnitine yields NADH as well as the transfer of electrons to electron-transferring flavoprotein (ETF), which supplies electrons to ubiquinone in the electron transport system through ETF-ubiquinone oxidoreductase (Perevoshchikova et al., 2013).

With no exogenous ADP to support oxidative phosphorylation, the steady state supported by glutamate, malate, succinate, and octanoylcarnitine (Figure 2) was characterized as leak-supported respiration (L). ADP (2.5 mM) was then added to stimulate ATP synthase and support respiration under phosphorylating conditions. The steady state that followed was characterized as oxidative phosphorylation-supported respiration (P). This state is analogous to the routine respiration (R) of intact cells. Cytochrome *c* (10 μ M), which is also a component of the electron transport system, was then added to assess the integrity of the outer mitochondrial membranes. Cytochrome *c* is a large protein that cannot penetrate an intact outer mitochondrial membrane. Therefore, any increase in oxygen consumption after cytochrome *c* administration would be indicative of damage to the mitochondrial membrane. Results from experiments in which respiration increased more than 10% in response to cytochrome *c* administration were discarded. Lastly, antimycin A (2.5 μ M) was added to account for ROX as in the protocol for intact cells.

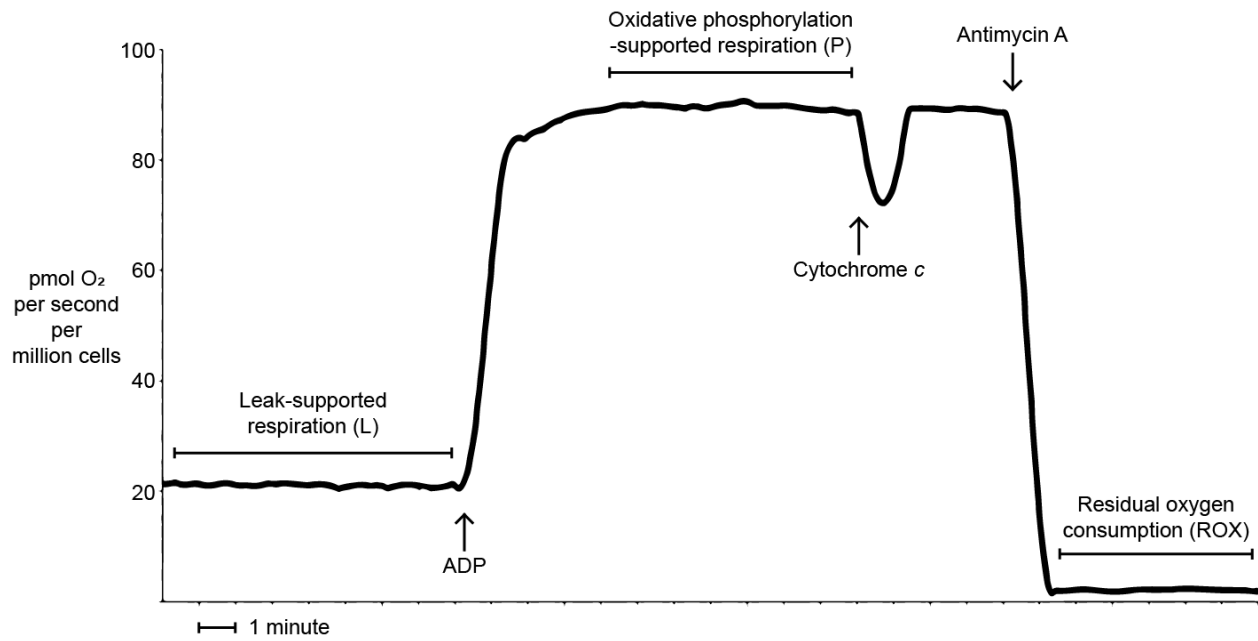


Figure 2. Annotated display from a permeabilized-cell respiration experiment.

^L Maintained by glutamate, malate, succinate, octanoylcarnitine, and proton leak.

^P Supported by glutamate, malate, succinate, octanoylcarnitine, and ADP.

^{ROX} Residual oxygen consumption after inhibition of complex III.

Hydrogen peroxide emission

Hydrogen peroxide emission was quantified simultaneously with respiration measurements (Krumschnabel et al., 2015; Makrecka-Kuka, Krumschnabel, and Gnaiger, 2015). After transferring pretreated cells to the respiratory chamber, horseradish peroxidase (1 U/mL) and Amplex UltraRed (10 μ M) were added followed by three 0.1 μ M steps of a hydrogen peroxide standard (40 μ M) to calibrate the instrument for fluorescence readings. Horseradish peroxidase catalyzes the reaction between hydrogen peroxide and Amplex UltraRed in a 1:1 stoichiometric ratio to form a fluorescent compound, resorufin, which exhibits excitation and emission wavelengths of 563 and 587 nm, respectively.

When exposed to a specific wavelength of light (563 nm), electrons within the chemical bonds of resorufin are transiently excited into higher-energy molecular orbitals. The eventual return of these electrons to their original orbitals causes a release of energy in the form of emitted light at a different wavelength (587 nm). The intensity of light at this emission wavelength can be detected and recorded. Based on the changes in emission intensity that occurred after multiple additions of the hydrogen peroxide standard, a slope was generated to relate the emission intensity to the concentration of hydrogen peroxide in the respiratory chamber. This slope was then used to convert any recorded emission intensity during an experiment into a rate of hydrogen peroxide appearance. Later assessments of hydrogen peroxide emission were performed in growth media that lacked pyruvate and phenol red in order to improve signal stability. Octanoylcarnitine (0.2 mM) was added during routine respiration in these later experiments to additionally stimulate electron transport in the absence of pyruvate. The media change was made due to the possibility that pyruvate, a known scavenger of hydrogen peroxide (Long and Halliwell, 2009), may have prevented the rate of hydrogen peroxide

emission from rising enough to generate detectable differences between treatments. Phenol red was removed as an additional precaution due to the possibility of its color interfering with the detection of changes in fluorescence intensity.

Treatments

During preliminary experiments, an increased rate of oxygen consumption and a decreased rate of hydrogen peroxide emission were observed when curcumin was added to cell-free media in the respiratory chamber. Such an effect only occurred when curcumin was added directly to the chamber in the presence of reagents for the Amplex Red assay and may have been a result of curcumin oxidation in the presence of horseradish peroxidase (Buchanan and Nicell, 1997; Nelson et al., 2017). In order to reduce the risk of curcumin-induced interference during hydrogen peroxide measurements, a pretreatment protocol was employed in which cells were treated and then washed prior to analysis. Such a pretreatment protocol could also yield more meaningful results than strictly measuring the respiration of cells in the presence of treatment. This is because pretreating the cells and then washing the cells prior to respiration analysis would show if the effects of treatment persist even after the treatment is removed.

The old culture media on cells was replaced with fresh media that was previously warmed to 37 °C and combined with treatment. After 30 minutes of incubation with treatment, cells were washed twice and harvested as previously described. The incubation time of 30 minutes was selected based on past experiments with C2C12 myotubes (Kang and Kim, 2010) where curcumin treatments between 30-60 minutes in length caused the greatest changes to metabolic pathway regulation compared with other incubation times.

Due to their poor solubility in water, treatments were dissolved in 100% DMSO and were prepared for a final concentration of 0.1% DMSO v/v in cell culture media. In past experiments

with isolated mitochondria, DMSO concentrations up to 2% had no effect on basal oxygen consumption (Martineau 2012). Comparisons between 0.1% DMSO-treated cells and untreated cells during preliminary experiments revealed no differences in respiration or hydrogen peroxide measurements. Treatments in the present study included curcumin (40 μ M), ursolic acid (0.12 μ M), a combination of curcumin plus ursolic acid (40 μ M and 0.12 μ M, respectively), and a vehicle control (0.1% DMSO).

Concentration selections were based on past experiments with isolated mitochondria. Martineau (2012) treated mitochondria from rat liver with a range of curcumin doses and found that during inhibition of ATP synthase, 40 μ M curcumin increased the rate of oxygen consumption to half of the rate observed during oxidative phosphorylation without treatment. Under similar conditions, Liobikas et al. (2011) treated mitochondria from rat heart with ursolic acid and found that a concentration of 50 ng/mL (\sim 0.12 μ M) also increased the rate of oxygen consumption during inhibition of ATP synthase to half of the rate observed during oxidative phosphorylation without treatment.

The concentrations of curcumin and ursolic acid that were used in the present study were additionally selected in order to reduce the risk of potential cytotoxic effects. In past experiments with C2C12 myotubes, a 24-hour incubation with 40 μ M curcumin (Kang and Kim, 2010) and a 72-hour incubation with up to 5 μ M ursolic acid (Figueiredo and Nader, 2012) had no effect on cell viability as assessed by MTT assay. Only living cells will reduce the yellow MTT compound to form formazan, a purple product (Plumb, Milroy, and Kaye, 1989). The light absorbance of samples treated with MTT can therefore be compared to determine relative levels of cell viability. Both Kang and Kim (2010) and Figueiredo and Nader (2012) saw the viability of cells decrease in response to more than 40 μ M curcumin or 5 μ M ursolic acid, respectively. The

cytotoxic effect of high curcumin doses on C2C12 myotubes was additionally noted in a study by Martineau (2012). While an 18-hour incubation with 50 μM curcumin had no effect on cell viability, treatment with 100 μM curcumin over the same duration led to myotube detachment from cell plates.

Coupling efficiency

The mitochondrial coupling efficiency of intact cells was based on the rates of oxygen consumption during routine respiration (R) and during leak-supported respiration (L) and was calculated as $[1 - (L/R)]$. For permeabilized cells, oxidative phosphorylation-supported respiration (P) was used in place of routine respiration, and the efficiency was calculated as $[1 - (L/P)]$. As a reminder, routine respiration (R) is supported by endogenous ADP while the oxidative phosphorylation-supported respiration (P) of permeabilized cells is maintained by exogenous ADP. Both of these conditions are analogous, however, and reflect the rate of oxygen consumption during phosphorylating conditions. The mitochondrial coupling efficiency indicates the fraction of oxygen consumption that is coupled to oxidative phosphorylation. Because the rate of oxygen consumption is controlled by electron-transport-system activity, values of mitochondrial coupling efficiency also reflect the degree of coupling between the electron transport system and oxidative phosphorylation. A value of 1 would indicate a completely coupled system (electron transport with no proton leak) while a value of 0 would indicate a completely uncoupled system (electron transport with no oxidative phosphorylation).

For a demonstration of how this works, consider a theoretical example with cells that exhibit a rate of oxygen consumption of 10 pmol/s during routine respiration. After inhibition of ATP synthase by the addition of oligomycin, this rate drops to 0 pmol/s, meaning that oxygen consumption completely ceased. This result implies that the electron transport system of these

cells was completely coupled to oxidative phosphorylation; without functional ATP synthase, no oxygen consumption took place. The value given by $[1-(L/R)]$ would be 1. On the other hand, consider if inhibition of ATP synthase had no effect on these cells and that their rate of oxygen consumption remained at 10 pmol/s cells after the addition of oligomycin. This would imply that the electron transport system within these cells was not linked (or was completely uncoupled) to ATP synthesis. The value given by $[1-(L/R)]$ would be 0. Reported mitochondrial coupling efficiency values vary widely by cell type (Thrush et al., 2013) and by method of assessment (Divakaruni and Brand, 2011), with some values in skeletal muscle ranging from 0.66 in rats (Rolfe et al., 1999) to over 0.90 in mice (Marcinek et al., 2004).

Statistics

The mean mitochondrial coupling efficiency of cells and rate of hydrogen peroxide emission during routine respiration of 4 treatment groups (vehicle, curcumin, ursolic acid, and combination) were analyzed by two-way analysis of variance in order to assess the interaction between curcumin and ursolic acid treatments. The mean results of the four treatment groups were also compared against each other using the Bonferroni method to assess differences between treatments. To reduce the risk of incorrectly rejecting a null hypothesis while performing multiple comparisons of means, the Bonferroni method applies a correction to the alpha level for individual comparisons within a family of statistical tests. Our desired alpha level of 0.05 for each family (mitochondrial coupling efficiency and hydrogen peroxide emission) was adjusted to 0.008 in order to account for six independent comparisons. These comparisons included vehicle to curcumin, vehicle to ursolic acid, vehicle to combination, curcumin to ursolic acid, curcumin to combination, and ursolic acid to combination. Remaining analyses were conducted by Student's *t*-test using an alpha level of 0.05.

RESULTS

Mitochondrial coupling efficiency

In order to accomplish the primary study objective of determining whether curcumin and ursolic acid decrease the mitochondrial coupling efficiency of intact skeletal muscle cells, C2C12 myoblasts were pretreated for 30 minutes and then subjected to respiration analysis in their intact state. The results of these 30-minute pretreatments on mitochondrial coupling efficiency are shown in Table 1. In addition, the rates of oxygen consumption that were used for calculations of efficiency are provided in Table 2. Curcumin ($-17.0 \pm 0.4\%$), ursolic acid ($+4.1 \pm 1.1\%$), and combined treatment ($-8.0 \pm 0.9\%$) each changed the mitochondrial coupling efficiency of cells relative to vehicle ($p < 0.008$). These relative changes are depicted in Figure 3. The mitochondrial coupling efficiencies that resulted from curcumin, ursolic acid, or combined treatment differed from each other as well ($p < 0.008$). Notably, curcumin and ursolic acid demonstrated opposite effects on mitochondrial coupling efficiency when used individually, and a subtractive effect was observed when these treatments were used in combination. This finding of no synergism also accomplished our objective to determine if curcumin and ursolic acid act synergistically to decrease the mitochondrial coupling efficiency of intact skeletal muscle cells.

Table 1. Mitochondrial coupling efficiency of intact C2C12 myoblasts after pretreatment.

Treatment	Mitochondrial coupling efficiency
Vehicle	0.78 ± 0.01 ^a
Curcumin	0.65 ± 0.003 ^b
Ursolic acid	0.81 ± 0.01 ^c
Combination	0.72 ± 0.01 ^d

The mitochondrial coupling efficiency describes the proportion of oxygen consumption that is coupled to ATP synthesis. Measurements were taken after a 30-minute pretreatment. Treatments included vehicle (0.1% DMSO), curcumin (40 μM), ursolic acid (0.12 μM), and combination (40 μM curcumin with 0.12 μM ursolic acid).

Treatments with different superscripts are different from each other, $p < 0.008$.

Data expressed as means ± SEM.

N = 6 per treatment.

Table 2. Rates of oxygen consumption of intact myoblasts after 30-minute pretreatment.

Treatment	R	L	ROX
Vehicle	8.2 ± 0.8	1.8 ± 0.1	2.5 ± 0.3
Curcumin	7.7 ± 1.0	2.7 ± 0.4	2.6 ± 0.3
Ursolic acid	10.7 ± 0.5	2.0 ± 0.1	3.1 ± 0.1
Combination	11.5 ± 1.3	3.3 ± 0.4	3.8 ± 0.2

Rates of oxygen consumption (pmol/s*million cells) of intact C2C12 myoblasts were measured during routine respiration (R), during leak-supported respiration (L), and after inhibition of the electron transport system (ROX) following a 30-minute pretreatment. Rates of oxygen consumption during R and L (shown here as ROX-corrected values) were used to calculate mitochondrial coupling efficiency. Treatments included vehicle (0.1% DMSO), curcumin (40 μM), ursolic acid (0.12 μM), and combination (40 μM curcumin with 0.12 μM ursolic acid). Data expressed as means ± SEM.

N = 6 per treatment.

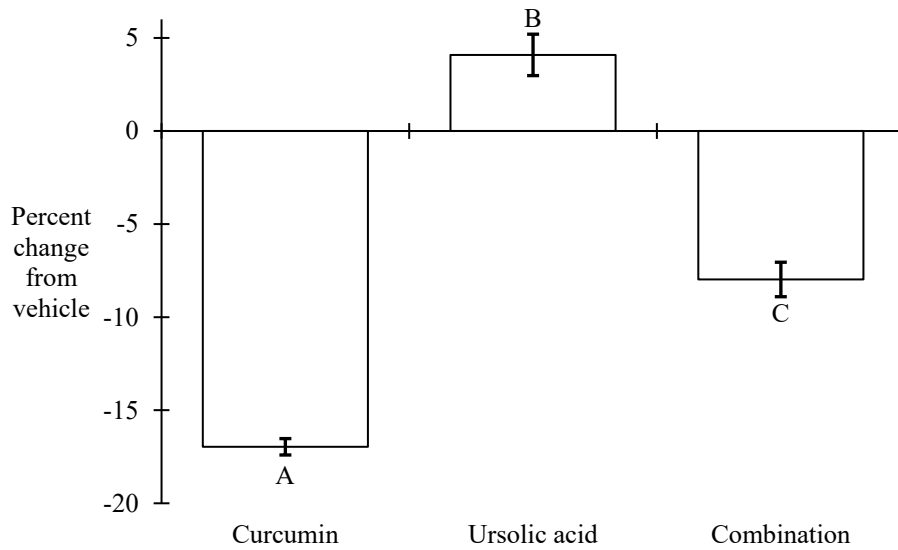


Figure 3. Mitochondrial coupling efficiency of intact C2C12 myoblasts.

The mitochondrial coupling efficiency describes the proportion of oxygen consumption that is coupled to ATP synthesis and was assessed after a 30-minute pretreatment. Treatments included vehicle (0.1% DMSO), curcumin (40 μ M), ursolic acid (0.12 μ M), and combination (40 μ M curcumin with 0.12 μ M ursolic acid).

Treatments with different letters are different from vehicle and from each other, $p < 0.008$.

Data expressed as means \pm SEM.

N = 6 per treatment.

Hydrogen peroxide emission

Another objective of the study was to determine if curcumin and ursolic decrease the rate of hydrogen peroxide emission from intact skeletal muscle cells. The results of 30-minute pretreatments on the rate of hydrogen peroxide emission from intact C2C12 myoblasts during routine respiration are shown in Table 3. A pattern similar to that of mitochondrial coupling efficiency was observed in that curcumin decreased the rate of hydrogen peroxide emission, ursolic acid increased the rate of emission, and the combined treatment produced a rate that was intermediate between the two individual treatments. These changes are depicted relative to vehicle in Figure 4. Even though the pattern of hydrogen peroxide emission mirrored our observed changes in mitochondrial coupling efficiency, the only difference in hydrogen peroxide emission that reached statistical significance ($p < 0.008$) occurred between curcumin and ursolic acid. The change between vehicle and curcumin approached statistical significance ($-43 \pm 8\%$ with curcumin relative to vehicle, $p = 0.013$), but a statistical difference could not be concluded after applying the Bonferroni correction. Similarly, no statistical differences were observed between vehicle and ursolic acid ($+25 \pm 7\%$ with ursolic acid relative to vehicle, $p > 0.1$), vehicle and combination ($-1 \pm 10\%$ with combination relative to vehicle, $p > 0.9$), curcumin and combination ($p = 0.014$), or ursolic acid and combination ($p > 0.09$). The finding of a non-significant increase in hydrogen peroxide emission with ursolic acid relative to vehicle accomplished our objective to determine if ursolic acid decreased the rate of hydrogen peroxide emission from intact skeletal muscle cells. Similarly, our finding of no synergism between curcumin and ursolic acid accomplished the objective of determining whether curcumin and ursolic acid act synergistically to decrease the rate of hydrogen peroxide emission from intact skeletal muscle cells.

Table 3. Rates of hydrogen peroxide emission from intact C2C12 myoblasts.

Treatment	R	L	ROX
Vehicle	0.38 ± 0.06 ^{ab}	0.40 ± 0.06 ^{ab}	0.49 ± 0.08 ^{ab}
Curcumin	0.22 ± 0.03 ^b	0.23 ± 0.02 ^b	0.30 ± 0.04 ^b
Ursolic acid	0.47 ± 0.03 ^a	0.50 ± 0.03 ^a	0.62 ± 0.04 ^a
Combination	0.37 ± 0.04 ^{ab}	0.41 ± 0.04 ^a	0.53 ± 0.05 ^a

Rates of hydrogen peroxide emission (pmol/s*million cells) from intact C2C12 myoblasts were assessed after a 30-minute pretreatment during routine respiration (R), during leak-supported respiration (L), and after inhibition of the electron transport system (ROX). Treatments included vehicle (0.1% DMSO), curcumin (40 μM), ursolic acid (0.12 μM), and combination (40 μM curcumin with 0.12 μM ursolic acid).

Treatments with different superscripts are different from each other, $p < 0.008$.

Data expressed as means ± SEM.

N = 6 per treatment.

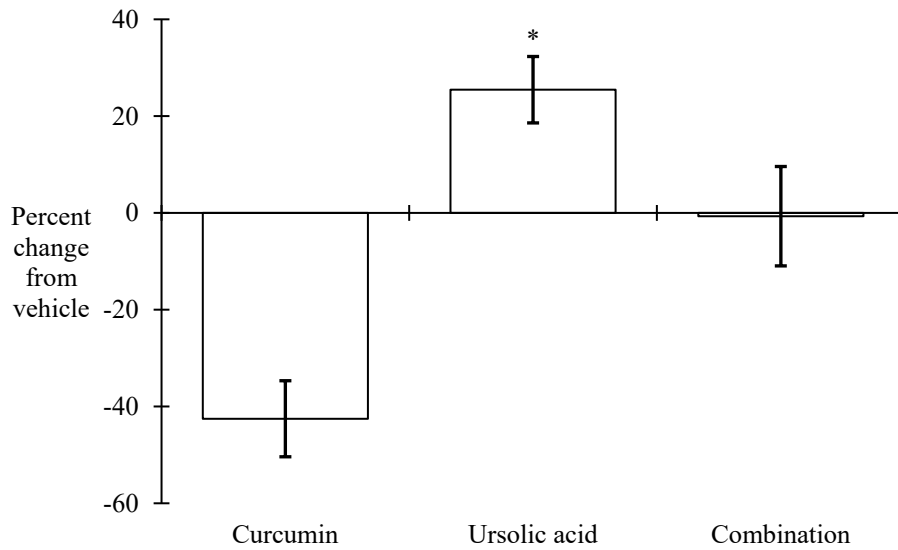


Figure 4. Rate of hydrogen peroxide emission from intact C2C12 myoblasts.

The rate of hydrogen peroxide emission was assessed during routine respiration after a 30-minute pretreatment. Treatments included vehicle (0.1% DMSO), curcumin (40 μ M), ursolic acid (0.12 μ M), and combination (40 μ M curcumin with 0.12 μ M ursolic acid).

* Different from curcumin, $p < 0.008$.

Data expressed as means \pm SEM.

N = 6 per treatment.

Experiments without pyruvate and phenol red

In attempt to detect a possible statistical difference in the rate of hydrogen peroxide emission between vehicle and curcumin, additional experiments were performed in growth media that lacked phenol red and that substituted octanoylcarnitine for pyruvate. This revised protocol was used in light of pyruvate's ability to neutralize reactive oxygen species (Long and Halliwell, 2009), which may have had prevented meaningful rises in hydrogen peroxide emission. Phenol red was also removed as an additional precaution in case its color had interfered with the detection of changes in fluorescence intensity. As shown in Table 4, mitochondrial coupling efficiency was again reduced by curcumin compared with vehicle in these experiments ($-11 \pm 1.1\%$, $p < 0.05$). The rates of oxygen consumption that were used for calculations of efficiency are also provided in Table 5.

Relative to vehicle, the rate of hydrogen peroxide emission from intact C2C12 myoblasts was reduced after curcumin pretreatment during routine respiration ($-43 \pm 13\%$, $p < 0.05$) as well as during all other stages of respiration ($p < 0.05$) in media that lacked pyruvate and phenol red (Table 6). The absolute rates of hydrogen peroxide emission were indeed higher in these experiments compared to earlier assessments with pyruvate and phenol red present. Interestingly, the mean percent change in hydrogen peroxide emission with curcumin relative to vehicle was the exact same in both experimental conditions albeit with greater variability when pyruvate and phenol red had been removed. The finding of a lower rate of hydrogen peroxide emission after curcumin treatment accomplished our objective to determine if curcumin reduces the rate of hydrogen peroxide emission from intact skeletal muscle cells.

Table 4. Mitochondrial coupling efficiencies of intact and permeabilized C2C12 myoblasts.

Treatment	MCE of intact cells ^a	MCE of permeabilized cells ^b
Vehicle	0.83 ± 0.02	0.79 ± 0.001
Curcumin	0.74 ± 0.01*	0.79 ± 0.005

The mitochondrial coupling efficiency (MCE) describes the proportion of oxygen consumption that is coupled to ATP synthesis. MCE was assessed after a 30-minute pretreatment. Treatments included vehicle (0.1% DMSO) and curcumin (40 μM).

^a Assessed in media without phenol red and with octanoylcarnitine in place of pyruvate.

^b Assessed in MiR05.

* Different from vehicle within the same cell model, $p < 0.05$.

Data expressed as means ± SEM.

N = 6 per treatment for intact cells and 3 per treatment for permeabilized cells.

Table 5. Rates of oxygen consumption of intact myoblasts in media without pyruvate.

Treatment	R	R'	L	ROX
Vehicle	10.4 ± 1.1	11.0 ± 1.2	1.9 ± 0.2	3.7 ± 0.2
Curcumin	7.8 ± 0.7	8.5 ± 0.9	2.2 ± 0.3	3.0 ± 0.2

Rates of oxygen consumption (pmol/s*million cells) of intact C2C12 myoblasts were measured during routine respiration (R), after the addition of octanoylcarnitine (R'), after the addition of oligomycin (L), and after inhibition of the electron transport system (ROX) in growth media that lacked pyruvate and phenol red after a 30-minute pretreatment. Rates of oxygen consumption during R' and L (shown here as ROX-corrected values) were used to calculate mitochondrial coupling efficiency. Treatments included vehicle (0.1% DMSO) and curcumin (40 uM).

* Different from vehicle within the same respiratory state, $p < 0.05$.

Data expressed as means ± SEM.

N = 6 per treatment.

Table 6. Rates of hydrogen peroxide emission from myoblasts in media without pyruvate.

Treatment	R	R'	L	ROX
Vehicle	0.86 ± 0.14	0.96 ± 0.16	0.99 ± 0.16	1.24 ± 0.19
Curcumin	0.49 ± 0.11*	0.56 ± 0.13*	0.57 ± 0.13*	0.73 ± 0.15*

Rates of hydrogen peroxide emission (pmol/s*million cells) from intact C2C12 myoblasts were assessed during routine respiration (R), after addition of octanoylcarnitine (R'), after addition of oligomycin (L), and after addition of antimycin A (ROX) in growth media that lacked pyruvate and phenol red after a 30-minute pretreatment.

Treatments included vehicle (0.1% DMSO) and curcumin (40 uM).

* Different from vehicle within the same respiratory state, $p < 0.05$.

Data expressed as means ± SEM.

N = 6 per treatment.

Immediate effect of curcumin treatment on rate of oxygen consumption

In order to observe the immediate effect of curcumin on the respiration of intact cells, curcumin was added to cell suspensions within the respiratory chamber. Assessment of hydrogen peroxide emission was not performed in these experiments due to previously observed reactions between curcumin and reagents in the Amplex Red assay. When added to intact C2C12 myoblasts in the respiratory chamber (Figure 5), curcumin abruptly increased the rate of oxygen consumption by $40 \pm 4\%$ versus a vehicle-induced change of $-1 \pm 1\%$ ($p < 0.05$ between treatments, Table 7). The rise in the rate of oxygen consumption peaked approximately 10 minutes after curcumin administration and reached a steady state thereafter. Curcumin treatment again led to reduced mitochondrial coupling efficiency in these experiments ($-12 \pm 2\%$ relative to vehicle, $p < 0.05$). Interestingly, the increased rate of oxygen consumption during routine respiration with curcumin ($+7.1 \text{ pmol/s} \cdot \text{million cells}$ relative to vehicle) was not completely accounted for by mitochondrial uncoupling (based on an increased rate of oxygen consumption of only $+3.4 \text{ pmol/s} \cdot \text{million cells}$ with curcumin relative to vehicle during leak-supported respiration). These findings relate to our objective of determining if curcumin decreases the mitochondrial coupling efficiency of intact skeletal muscle cells by showing that curcumin's effect on the rate of oxygen consumption occurred abruptly and peaked within 10 minutes after initiating treatment.

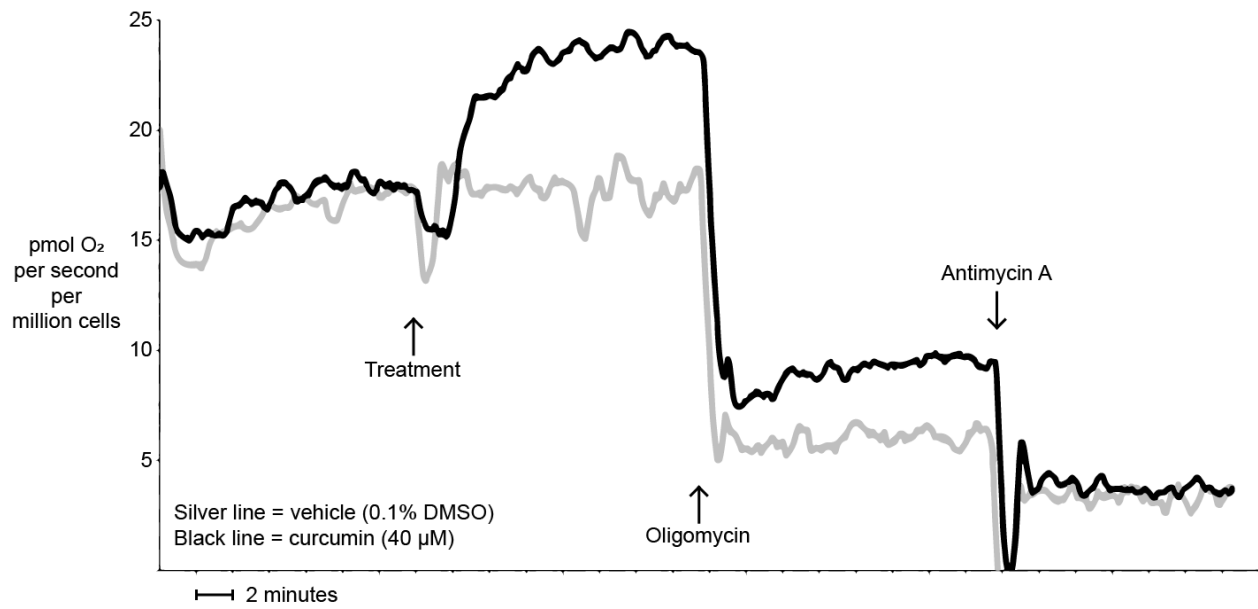


Figure 5. Annotated results of two simultaneous experiments with intact C2C12 myoblasts. Rate of oxygen (O₂) consumption (pmol/s*million cells) was measured during two simultaneous experiments with intact C2C12 myoblasts. Treatments and reagents were added to cell suspensions at the points indicated by arrows.

Table 7. Mitochondrial respiration of intact C2C12 myoblasts in the presence of treatment.

Treatment	R	R ^T	L ^T	ROX ^T	MCE ^T
Vehicle	15.3 ± 0.7	15.1 ± 0.6	2.9 ± 0.1	3.5 ± 0.1	0.81 ± 0.01
Curcumin	16.0 ± 1.4	22.2 ± 1.4*	6.3 ± 0.1*	4.1 ± 0.2*	0.71 ± 0.02*

Rates of oxygen consumption (pmol/s*million cells) of intact C2C12 myoblasts were assessed during routine respiration (R), during leak-supported respiration (L), and after inhibition of the electron transport system (ROX) immediately before and after the addition of treatment to cells in the respiratory chamber. Rates of oxygen consumption during R and L (shown here as ROX-corrected values) were used to calculate mitochondrial coupling efficiency (MCE), which describes the proportion of oxygen consumption that is coupled to ATP synthesis.

^T In the presence of treatment: vehicle (0.1% DMSO) or curcumin (40 μM).

* Different from vehicle, p < 0.05.

Data expressed as means ± SEM.

N = 4 per treatment.

Permeabilization of cells after 30-minute pretreatment

We next sought to determine if the effect of curcumin pretreatment on mitochondrial coupling efficiency would persist if cells were permeabilized. This information is important to know because muscle tissue samples from humans and animals are normally assessed in the permeabilized condition (Pesta and Gnaiger, 2012). Since this model of assessment is different from the intact condition used in our experiments up to this point, we were curious if the effects of curcumin pretreatment on the mitochondrial coupling efficiency of intact cells could still be seen after permeabilization of their cell membranes. To our surprise, no difference in mitochondrial coupling efficiency was observed between vehicle- and curcumin-pretreated C2C12 myoblasts after cell membrane permeabilization ($p > 0.7$, Table 4, with rates of oxygen consumption that were used to calculate efficiency provided in Table 8). This finding is of critical value for future experiments involving curcumin administration to humans or animals. If the mitochondrial coupling efficiency of skeletal muscle tissue from subjects in these experiments is assessed after permeabilization, researchers may falsely conclude that curcumin had no effect. In reality, an effect may have been present but was lost or went undetected after samples were permeabilized.

Table 8. Rates of oxygen consumption of pretreated myoblasts after permeabilization.

Treatment	L	P	ROX
Vehicle	14.4 ± 1.8	68.3 ± 8.3	1.2 ± 0.5
Curcumin	13.9 ± 2.6	66.3 ± 10.7	1.5 ± 0.3

Rates of oxygen consumption (pmol/s*mL) of pretreated C2C12 myoblasts were measured in the permeabilized condition during leak-supported respiration (L), during oxidative phosphorylation-supported respiration (P), and after inhibition of the electron transport system (ROX). Rates of oxygen consumption during L and P (shown here as ROX-corrected values) were used to calculate mitochondrial coupling efficiency. Treatments included vehicle (0.1% DMSO) and curcumin (40 μM).

Data expressed as means ± SEM.

N = 3 per treatment.

DISCUSSION

Objectives

The main objective of this study was to determine if curcumin decreases the mitochondrial coupling efficiency and hydrogen peroxide emission of intact skeletal muscle cells. We found that curcumin lowered the mitochondrial coupling efficiency of intact C2C12 myoblasts after a 30-minute pretreatment on two separate occasions, and we observed that curcumin reduced the mitochondrial coupling efficiency of cells when they were treated directly within the respiratory chamber as well. Additional experiments showed that curcumin also reduced the rate of hydrogen peroxide emission from these cells. These results provide evidence for how curcumin treatment may have improved the blood glucose control and insulin sensitivity of subjects during clinical investigations in the past (Chuengsmarn et al., 2012; Na et al., 2013; Chuengsmarn et al., 2014).

Another objective was to determine if curcumin and ursolic acid would act synergistically to reduce the mitochondrial coupling efficiency and hydrogen peroxide emission of intact skeletal muscle cells. Such synergism could improve therapies involving curcumin by allowing a lower curcumin dose to be used to improve insulin sensitivity and blood-glucose management. We were surprised to find that ursolic acid independently increased the mitochondrial coupling efficiency of intact C2C12 myoblasts and caused a statistically nonsignificant increase in the rate of hydrogen peroxide emission. When curcumin and ursolic acid were used in combination, the effects of curcumin on mitochondrial coupling efficiency and hydrogen peroxide emission were attenuated. These results show that further research will be necessary to determine how curcumin and ursolic acid may have different effects on these variables despite having independently improved blood-glucose control and insulin sensitivity in past studies.

Past studies of curcumin and glucose uptake

The effect of curcumin on stimulating glucose uptake in skeletal muscle cells has previously been well-established in a number of experimental models (Kim et al., 2010; Na et al., 2011) including C2C12 cells. Martineau (2012) treated C2C12 myotubes with curcumin (25 and 50 μM) for 18 hours. While 25 μM curcumin did not have a significant effect, 50 μM curcumin caused an approximately 60% increase in rate of glucose uptake relative to vehicle. Kang and Kim (2010) treated C2C12 myotubes for one hour with curcumin (3, 10, and 40 μM) and observed the greatest rate of glucose uptake with 40 μM curcumin compared to vehicle. Molecular signaling pathways involving AMP-activated protein kinase (AMPK) and acetyl-CoA carboxylase (ACC) were also assessed in their experiments. AMPK is centrally involved in the regulation of many metabolic pathways (Hardie, Ross, and Hawley, 2012). It is phosphorylated and activated in response to increased levels of AMP (the degradation product of ATP and an indicator of increased cellular energy demand). Not surprisingly, AMPK activation also occurs when coupling between the electron transport system and oxidative phosphorylation is impaired (Gates et al., 2007; Keipert et al., 2013). A main effect of AMPK activation is the increased translocation of the insulin-sensitive glucose transporter GLUT4 from the cytosol to the plasma membrane of cells. With more GLUT4 in the plasma membrane, the cell's capacity to obtain glucose from the blood is increased. Another effect of AMPK activation is the phosphorylation, or inactivation, of ACC—an enzyme that catalyzes the initial step of fatty acid synthesis from acetyl-CoA (Hardie, 2014). By so doing, acetyl-CoA is directed toward immediate oxidation and ATP production instead of being sequestered during times of urgent energy need. Kang and Kim (2010) measured AMPK activation and ACC inactivation in response to one hour of curcumin treatment. The ratios of phosphorylated AMPK (p-AMPK)/AMPK and phosphorylated ACC (p-

ACC)/ACC both were both increased after incubation with 30 μ M curcumin and were even greater after treatment with 40 μ M curcumin. By treating cells with 40 μ M curcumin over various time points ranging from 30 minutes to 12 hours, they found that p-AMPK/AMPK and p-ACC/ACC both peaked between 30-60 minutes of treatment and gradually declined thereafter while still remaining elevated through 12 hours of treatment relative to vehicle. They also observed that a 30-minute incubation with dorsomorphin (20 μ M), an AMPK inhibitor, abolished the effect of a one-hour treatment with curcumin (40 μ M) on stimulating glucose uptake.

In summary, an insulin-independent increase in glucose uptake has been observed after curcumin treatment, and this increase appeared to depend on the activation of AMPK. Our finding of decreased mitochondrial coupling efficiency in response to curcumin, shown for the first time in intact skeletal muscle cells, provides evidence for why AMPK may be activated during curcumin treatment. This may occur because reduced coupling between the electron transport system and oxidative phosphorylation leads to impaired cellular energy production and increases the amount of fuel that is required to maintain optimal ATP levels (Thrush et al., 2013). This could be confirmed if maintenance of mitochondrial coupling efficiency before and during curcumin treatment prevents AMPK activation.

Curcumin and insulin sensitivity

Along with directly stimulating glucose uptake through increased activation of AMPK, curcumin treatment in past studies also improved the glucose-uptake response to insulin. Kang and Kim (2010) incubated C2C12 myotubes with curcumin (40 μ M) or insulin (100 nM) for one hour and then assessed the quantity of GLUT4 protein in the cytosolic and membrane fractions of the cells. Both treatments led to increased GLUT4 content in the membrane fractions.

Interestingly, the combined treatment with curcumin (40 μM) and insulin (100 nM) for one hour led to an increased membrane fraction of GLUT4 that was even greater than the additive effects of each individual treatment. This finding provided evidence that curcumin increases the insulin-mediated translocation of GLUT4 to the cell membrane in addition to stimulating GLUT4 translocation through an insulin-independent mechanism (possibly through AMPK activation as described previously). Deng et al. (2012) also investigated the effects of curcumin on insulin action. They first incubated C2C12 myotubes for 30 minutes with 0.5 μM tetradecanoylphorbol acetate (TPA), an activator of protein kinase C, which phosphorylates serine residues on IRS1 to induce a state of insulin resistance. Cells were additionally treated with insulin (100 nM) for 10 minutes then incubated with curcumin (1-40 μM) for three hours. The researchers found that curcumin decreased the serine phosphorylation of IRS1 in a dose-dependent manner and increased the activation of protein kinase B (Akt), a downstream effector of IRS1 within the insulin signal cascade. In an additional model, the researchers incubated C2C12 myotubes with palmitate (0.75 mM) for 16 hours to induce insulin resistance. Cells were then treated with curcumin (10 and 20 μM) for three hours and were afterward stimulated for 10 minutes with insulin (100 nM). The serine phosphorylation of IRS1 was again reduced by curcumin compared to vehicle in these experiments.

In light of the relationship between energy balance, redox environment, and insulin signaling (Fisher-Wellman and Neuffer, 2012), our novel findings that curcumin decreased the mitochondrial coupling efficiency and hydrogen peroxide emission of intact skeletal muscle cells support a possible mechanism underlying curcumin's benefit on insulin signaling. The increased fuel demand that results from uncoupling between the electron transport system and oxidative phosphorylation would cause any accumulation of reducing equivalents in the mitochondria to be

dissipated in order to maintain ATP production (Fisher-Wellman and Neuffer, 2012; Muoio and Neuffer, 2012). The likelihood of electrons uniting with oxygen prematurely would be decreased, and the production of reactive oxygen species would be reduced as well (Mailloux, 2015). A decreased level of reactive oxygen species would likewise lead to reduced phosphorylation of inhibitory serine and threonine residues on IRS proteins, and the propagation of the insulin signal cascade would be enhanced (Carnagarin, Dharmarajan, and Dass, 2015).

The potential link between our finding of reduced mitochondrial coupling efficiency after curcumin treatment and the past observations of improved insulin sensitivity after curcumin ingestion relates to energy balance. Assuming that energy intake remains constant, lower coupling between the electron transport system and oxidative phosphorylation could shift energy balance in a negative direction and lead to weight loss as more fuel will be required to maintain ATP levels (Harper, Green, and Brand, 2008; Tseng, Cypess, and Kahn, 2010). Such an effect from curcumin treatment is supported by past experiments in which body weight was measured over the course of habitual curcumin ingestion (Ejaz et al., 2009; Chuengsmarn et al., 2012). In a study by Chuengsmarn et al. (2012), human subjects consumed 1.5 grams of curcumin extract or placebo per day for nine months. No differences in body weight were detected between treatment groups during the first six months of the study. But by nine months, the group that ingested curcumin had experienced an average weight loss of 3.9 kg while the placebo group did not lose weight. A limitation to determining the mechanism for this weight loss, however, is that energy intake and expenditure were not assessed during the investigation. In another study, Ejaz et al. (2009) fed mice either a low-fat diet, a high-fat diet, or a high-fat diet supplemented with curcumin (500 mg/kg) for 12 weeks. No differences in food intake were detected between treatment groups. At the end of the study, mice on the high-fat diet weighed more than controls

while the weight gain of the curcumin group was attenuated. Although this difference may be attributed to different levels of physical activity, which were not measured during the study, the possibility remains that reduced mitochondrial coupling efficiency may have led to a greater fuel demand that prevented additional weight gain among the mice that ingested curcumin.

The relationship between hydrogen peroxide production and insulin sensitivity has previously been illustrated using experiments with animals (Anderson et al., 2009; Lee et al., 2010). For example, Anderson et al. (2009) fed rats a high-fat diet for 6 weeks and observed increased hydrogen-peroxide emission in the skeletal muscle of these animals as well as impaired whole-body insulin sensitivity compared to rats on a standard diet. Administration of a cell-permeable antioxidant to a subgroup of rats on the high-fat diet prevented any measurable increase in hydrogen-peroxide emission and preserved insulin sensitivity. While rats in the high-fat diet group also exhibited impaired protein kinase B activation (evidence of reduced insulin-signal propagation) in response to glucose challenge, the subgroup receiving antioxidant treatment showed no impairment compared to rats on the standard diet. In another model, the same researchers developed a transgenic strain of mice that overexpressed the human catalase gene in the mitochondria of their heart and skeletal muscle. Catalase is an enzyme that catalyzes the decomposition of hydrogen peroxide into water and oxygen. After feeding both wildtype and transgenic mice a high-fat diet for 12 weeks, the researchers observed significantly lower hydrogen-peroxide emission from the skeletal muscle of these animals relative to wildtype controls. The transgenic mice also displayed significantly higher rates of insulin-stimulated glucose uptake compared to their wildtype counterparts.

Although there is clearly a link between hydrogen peroxide emission and insulin sensitivity, we cannot conclude whether the lower hydrogen peroxide emission that was

observed after curcumin treatment in our study was due more to reduced mitochondrial coupling efficiency or to curcumin's intrinsic radical-scavenging tendency (Ak and Gülçin, 2008). Nonetheless, our finding that curcumin reduced the hydrogen peroxide emission of intact skeletal muscle cells is valuable when considering that skeletal muscle accounts for the majority of insulin-stimulated glucose uptake (Baron et al., 1988; DeFronzo and Tripathy, 2009). Since increased production of reactive oxygen species in skeletal muscle is associated with impaired insulin signaling (Di Meo, Iossa, and Venditti, 2017), our observation of reduced hydrogen peroxide emission from intact skeletal muscle cells lends possible evidence for how curcumin may have improved the insulin sensitivity of humans and animals in past studies (El-Moselhy et al., 2011; Na et al., 2011; Chuengsmarn et al., 2012; Na et al., 2013; Chuengsmarn et al., 2014).

Ursolic acid

In the present study, ursolic acid did not decrease the mitochondrial coupling efficiency of intact C2C12 myoblasts. A small but statistically significant increase in mitochondrial coupling efficiency was instead observed. This finding is in contrast to the results of Liobikas et al. (2012) who observed uncoupling between electron transport and oxidative phosphorylation in isolated heart mitochondria that were treated with ursolic acid. Our conflicting results may have been due to our use of a different model that involved intact cells instead of isolated mitochondria. In addition, the cells in our study were a model of skeletal muscle while the mitochondria used by Liobikas et al. (2012) were isolated from heart tissue. Different findings in different tissues types, even when the same treatment is used, is not uncommon (Gibellini et al., 2015). For example, curcumin has been reported to increase the activity of ATP synthase in mitochondria isolated from rat liver (Lim, Lim, and Wong, 2009) while a similar concentration

of curcumin decreased the activity of ATP synthase in mitochondria isolated from rat brain (Zheng and Ramirez, 2000).

Although the result of ursolic acid treatment on the mitochondrial coupling efficiency of intact C2C12 myoblasts was not as we hypothesized, this finding is supported by our observation that ursolic acid treatment trended toward causing a higher rate of hydrogen peroxide emission. Increased mitochondrial coupling efficiency means that less fuel is required to produce a given amount of ATP. Such an effect could exacerbate any accumulation of reducing equivalents within mitochondria because less fuel would be required to maintain ATP levels. As more reducing equivalents accumulate in the mitochondria, electrons are more likely to leave the transport system and unite with oxygen prematurely to form reactive oxygen species (Muoio and Neuffer, 2012).

While our findings from ursolic acid treatment do not support our proposed mechanism for ursolic acid's insulin-sensitizing properties, our results do coincide with the reported effects of ursolic acid on muscle growth (Kunkel et al., 2011; Jia et al., 2015) and exercise tolerance (Kunkel et al., 2012). Jia et al. (2015) orally administered ursolic acid (50-200 mg/kg body weight) to mice for eight weeks and found a dose-dependent increase in the skeletal muscle mass of mice that received ursolic acid compared to controls. Similarly, Kunkel et al. (2011) fed mice either a standard diet or a diet supplemented with 0.27% ursolic acid for five weeks and noted greater quadriceps weight, forearm muscle weight, triceps fiber diameter, and grip strength in the mice that received ursolic acid compared to those on the unsupplemented diet. In a follow-up study, the same research group (Kunkel et al., 2012) fed mice either a standard diet or a diet with 0.14% ursolic acid. They again observed muscle hypertrophy and increased strength in the mice that consumed ursolic acid compared to mice on the control diet. In addition, the mice that

consumed ursolic acid exhibited a higher exercise capacity relative to mice on the control diet; the mice that consumed ursolic acid ran a greater distance before exhaustion. These results are consistent with our finding that ursolic acid increased the mitochondrial coupling efficiency of intact C2C12 myoblasts because such an increase would reduce the fuel requirement needed to maintain optimal levels of ATP.

With greater coupling between the electron transport system and oxidative phosphorylation, more ATP will be produced per unit of fuel (Conley, 2016). Available fuel can then be spared for less-critical cellular functions such as muscle growth or adaptations to exercise. During times of increased energy demand, such as when exercising, fuel storage would also be used more efficiently so that ATP levels are maintained over a longer duration. These concepts are supported by the observations of Schlagowski et al. (2014) who treated rats for 21 days with 2,4-dinitrophenol, an established mitochondrial uncoupler, and noted lower body weights and decreased maximal running speeds in the treated animals compared to untreated controls. Conley et al. (2013) likewise found an association between decreased mitochondrial coupling efficiency and impaired exercise performance in elderly human subjects.

Synergism

Contrary to our hypothesis, we did not observe any synergism between curcumin and ursolic acid on the mitochondrial coupling efficiency and hydrogen peroxide emission of intact skeletal muscle cells. In fact, our data indicated a subtractive effect when intact C2C12 myoblasts were treated with both compounds in combination. Synergistic effects were originally hypothesized due to previously established findings that these compounds independently improved blood glucose management and insulin sensitivity (Jang et al., 2009; Chuengsmarn et al., 2012; Kunkel et al., 2012; Na et al., 2013; Chuengsmarn et al., 2014; Li et al., 2014; Jia et al.,

2015). Recent research also indicated synergism between curcumin and ursolic acid during the treatment of prostate cancer in mice (Lodi et al., 2017). While each compound alone had no effect on prostate tumors, a combined treatment with curcumin and ursolic acid led to decreased tumor size. Interactions between these compounds may have also affected mitochondrial coupling efficiency since reduced mitochondrial coupling was previously identified as a potential contributor to chemotherapeutic success (Marín-Prida et al., 2017). The effects curcumin and ursolic acid together on mitochondrial coupling efficiency and hydrogen peroxide emission, however, had not previously been assessed.

The discrepancy between our results and those of Lodi et al. (2017) may again be due to our use of a different model. Cancer cells in particular have been observed to respond differently to curcumin compared to nonmalignant cells (Ravindran, Prasad, and Aggarwal, 2009; Sordillo and Helson, 2015). For example, Kunwar et al. (2008) examined the uptake of curcumin into a variety of cell lines and noted the greatest uptake in malignant epithelial cells. The curcumin uptake by these cells was up to eight times higher than that of noncancerous varieties. Such a difference in the cellular uptake of curcumin and ursolic acid by our C2C12 myoblasts compared to prostate tumor cells may have contributed to the differences in observed synergism between our group and Lodi et al. (2017). The lack of synergism in our study is, however, consistent with our finding that curcumin and ursolic acid exerted opposite effects on the mitochondrial coupling efficiency and hydrogen peroxide emission of C2C12 myoblasts.

Permeabilization and mechanistic insights

An important finding of the present study was the lack of difference in mitochondrial coupling efficiency between vehicle- and curcumin-treated cells after permeabilization of cell membranes. This is significant for future assessments of skeletal muscle respiration after

curcumin consumption by humans or animals. Standard protocols for measuring respiration in skeletal muscle tissue involve permeabilization of fiber bundles (Pesta and Gnaiger, 2012). This permeabilization is not entirely intentional; when teasing apart the fiber bundles, which is necessary to ensure that oxygen diffusion across the tissue does not limit respiration, some partial permeabilization occurs in the fibers (Pesta and Gnaiger, 2012). Additional permeabilization may occur during the simple act of sample biopsy (Pesta and Gnaiger, 2012). Normally, the mechanical permeabilization that takes place during these processes is not a problem because samples are chemically permeabilized later to allow greater access of exogenous substrates to mitochondria during analysis of specific mitochondrial complexes. Partial membrane permeabilization poses a problem for the measurement of routine respiration, however, because an intact plasma membrane is necessary to accurately assess the respiration of cells in their native environment.

The requirement for cell membranes to be intact during analysis of routine respiration is likely due to the perturbed intracellular cellular calcium balance that occurs with plasma membrane damage (Orrenius, Gogvadze, and Zhivotovsky, 2015). Calcium concentrations are strictly regulated within cells, and increased intracellular calcium levels are damaging to mitochondria (Gnaiger et al., 2000; Lemasters et al., 2009). Indeed, the inadvertent membrane damage that occurs during sample preparation is considered a major obstacle to the assessment of routine respiration of muscle tissue (Pesta and Gnaiger, 2012). However, measurements of routine respiration could be attainable if sample preparations are performed carefully enough to preserve the plasma membrane integrity of the muscle fibers (Li et al., 2016). Care should therefore be taken to ensure that the plasma membranes of muscle samples remain intact during experiments that involve curcumin feeding and assessment of mitochondrial coupling efficiency.

Otherwise, those who conduct the research may falsely conclude that curcumin ingestion does not alter the mitochondrial coupling efficiency of skeletal muscle; such changes may indeed have been present but may have been abolished or rendered undetectable during permeabilization.

Our finding of no difference in mitochondrial coupling efficiency between vehicle- and curcumin-treated cells after permeabilization is peculiar, however, and is not entirely consistent with past experiments. Both Lim, Lim, and Wong (2009) and Martineau (2012) administered curcumin to isolated mitochondria and observed decreased coupling between electron transport and oxidative phosphorylation using similar concentrations to our study. An intact plasma membrane was clearly not necessary for curcumin to affect mitochondrial coupling in their experiments. However, these experiments were conducted in the presence of curcumin while our experiments followed a different pattern of treatment followed by washing of cells before analysis. Kunwar et al. (2008) previously assessed the cellular uptake and subcellular distribution of curcumin in MCF7 cells (an epithelial tumor cell line) and noted that approximately 55% of intracellular curcumin was localized in the membrane fraction. Other amounts included 25% in the cytosolic fraction, 17% in the nuclear fraction, and 3% in the mitochondrial fraction. Assuming a similar distribution in other cell types, the concentration of curcumin that the isolated mitochondria were exposed to in past studies (Lim, Lim, and Wong, 2009; Martineau, 2012) may have been much higher than what they would have experienced in their native cellular environment. The varied subcellular distribution of curcumin noted by Kunwar et al. (2008) also supports the possibility that barring direct mitochondrial exposure to high curcumin levels, a host of cellular signaling pathways and/or proteins may mediate curcumin's effect on the mitochondrial coupling efficiency of intact cells. Permeabilization of cell membranes may very well have impaired these intracellular interactions by disrupting cell homeostasis.

The apparent abolishment of changes to the mitochondrial coupling efficiency of pretreated cells after permeabilization is consistent with a possible mechanism for curcumin's uncoupling effect. In some (Morin et al., 2001; Ligeret et al., 2004), but not all (Lim, Lim, and Wong, 2009) past experiments in which the effects of curcumin on isolated mitochondria from rat liver were studied, curcumin appeared to induce the opening of the mitochondrial permeability transition pore (mPTP). The exact molecular nature of the mPTP is still debated (Biasutto et al., 2016). Current hypotheses support the mPTP as a voltage-sensitive channel that forms either within the ATP synthase complex (Alavian et al., 2014) or at the interface between ATP synthase dimers (Giorgio et al., 2013). In either case, opening of the mPTP is associated with the loss of mitochondrial membrane potential (or dissipation of the proton gradient across the inner mitochondrial membrane) and impaired production of ATP (Bernardi et al., 2015).

Extreme or prolonged opening of the mPTP contributes to mitochondrial injury through loss of mitochondrial proteins and mitochondrial equilibration with the external osmotic environment (Bernardi et al., 2015). These results of mPTP activation may also lead to cell death. Indeed, the activation of the mPTP has been implicated as a contributor to curcumin's chemotherapeutic effects (Qiu et al., 2014). The opening of the mPTP is, however, reversible (Jones et al., 2015), and may occur transiently in response to a number of variables including altered calcium concentrations, oxidative stress, pH environment, and hexokinase II (HKII) activity (Petronilli et al., 1999; Rasola et al., 2010; Korge et al., 2011; Bernardi et al., 2015). Such transient openings will not necessarily lead to cell death so long as a sufficient amount of mitochondrial solutes such as NADH and TCA cycle enzymes are retained in order to permit mitochondrial membrane repolarization (Biasutto et al., 2016).

Our finding of no difference between vehicle- and curcumin-pretreated cells after permeabilization may be reconciled to results from past experiments with isolated mitochondria (Lim, Lim, and Wong, 2009; Martineau, 2012) by the role of HKII in mPTP opening. HKII is a glycolytic enzyme that is localized on the mitochondrial outer membrane (Bernardi et al., 2015). When HKII is phosphorylated by Akt, the localization of HKII to the membrane is promoted (Miyamoto, Murphy, and Brown, 2008). Binding between HKII and the membrane is also facilitated through phosphorylation (inactivation) of glycogen synthase kinase 3 β (GSK3 β) by Akt (Robey and Hay, 2006; Ohori et al., 2008) as the activated form of GSK3 β will disrupt HKII's membrane-interaction by phosphorylating the membrane sites to which HKII normally binds (Pastorino, Hoek, and Shulga, 2005). Interestingly, curcumin was previously shown to induce HKII dissociation from the membrane through modulation of Akt signaling (Wang et al., 2015). This is significant because detachment of HKII from the mitochondrial outer membrane has been established as an activator of mPTP opening (Chiara et al., 2008).

When isolated mitochondria were previously treated with curcumin (Morin et al., 2001; Ligeret et al., 2004; Lim, Lim, and Wong, 2009; Martineau, 2012), the curcumin concentration experienced by the mitochondria may have been high enough to directly promote detachment of HKII from the outer mitochondrial membrane and induce mitochondrial uncoupling through mPTP opening. Reduced mitochondrial coupling efficiency may not have been observed in our experiments after permeabilization of pretreated cells because the intracellular distribution of curcumin to mitochondria is very low (Kunwar et al., 2008) and may have been too low to affect HKII directly. In our intact cells, however, the reduced efficiency seen with curcumin treatment may have been due to modulation of the Akt-HKII signaling pathway. The loss of such an effect would therefore come as no surprise as intracellular signaling is disrupted by permeabilization.

Further application to curcumin's reported effects *in vivo*

As we observed reduced mitochondrial coupling efficiency and hydrogen peroxide emission of intact skeletal muscle cells after curcumin treatment in our study, the possibility exists that similar effects may have contributed to the improved insulin sensitivity and blood glucose control of human subjects in past trials. Such a connection is limited, however, by the poor bioavailability of curcumin (Liu et al., 2016; Mirzaei et al., 2017). Reported serum concentrations of curcumin after oral ingestion are typically very low and are much lower than the concentrations used in our experiments. Researchers in one study reported the maximum serum curcumin concentration after consumption of 8g curcumin by human subjects to be only 1.7 μM (Cheng et al., 2001). Despite this low bioavailability, curcumin is widely distributed in tissues after ingestion, and detectable levels were shown to persist for up to 96 hours after a single oral dose of 500 mg/kg in rats (Suresh and Srinivasan, 2010). The possibility therefore exists for tissue accumulation of curcumin during habitual curcumin consumption, perhaps to a high enough degree to reduce mitochondrial coupling efficiency and hydrogen peroxide emission comparable to the findings of our study.

CONCLUSION

In summary, we demonstrated that curcumin decreased the mitochondrial coupling efficiency and reduced the rate of hydrogen peroxide emission of intact skeletal muscle cells. The addition of curcumin caused an abrupt increase in the rate of oxygen consumption during routine respiration, and this increase in oxygen consumption also persisted during leak-supported respiration. Contrary to our hypothesis, ursolic acid increased mitochondrial coupling efficiency and attenuated curcumin's effects when the two compounds were used in combination. Also, no change to mitochondrial coupling efficiency was observed after permeabilizing the cell membranes of curcumin-pretreated cells. While many studies have established that curcumin increases the glucose uptake and insulin sensitivity of skeletal muscle cells, our results shed light on how curcumin may exert these beneficial effects. Further research will be necessary to determine if the alterations to mitochondrial function that were identified in our study are indeed causing the improved insulin sensitivity and blood-glucose management seen with curcumin treatment during past investigations. In addition, our finding regarding permeabilization of cells reveals an important consideration for future studies of mitochondrial respiration in response to curcumin consumption. Unless cells are assessed in their intact state, changes to mitochondrial coupling efficiency may go unnoticed.

REFERENCES

- Adjeitey CN, Mailloux RJ, deKemp RA, Harper M. Mitochondrial uncoupling in skeletal muscle by UCP1 augments energy expenditure and glutathione content while mitigating ROS production. *Am J Physiol-Endoc M.* 2013;305:E405-E415.
- Affourtit C. Mitochondrial involvement in skeletal muscle insulin resistance: A case of imbalanced bioenergetics. *BBA-Bioenergetics.* 2016;1857:1678-1693.
- Aguirre V, Uchida T, Yenush L, Davis R, White MF. The c-Jun NH2-terminal kinase promotes insulin resistance during association with insulin receptor substrate-1 and phosphorylation of Ser307. *J Biol Chem.* 2000;275:9047-9054.
- Ak T, Gülçin İ. Antioxidant and radical scavenging properties of curcumin. *Chem-Biol Interact.* 2008;174:27-37.
- Alavian KN, Beutner G, Lazrove E, Sacchetti S, Park HA, Licznerski P, Li H, Nabili P, Hockensmith K, Graham M, Porter GA. An uncoupling channel within the c-subunit ring of the F1FO ATP synthase is the mitochondrial permeability transition pore. *Proc Natl Acad Sci USA.* 2014;111:10580-10585.
- Anderson EJ, Lustig ME, Boyle KE, et al. Mitochondrial H₂O₂ emission and cellular redox state link excess fat intake to insulin resistance in both rodents and humans. *J Clin Invest.* 2009;119:573-581.
- Anderson EJ, Yamazaki H, Neuffer PD. Induction of endogenous uncoupling protein 3 suppresses mitochondrial oxidant emission during fatty acid-supported respiration. *J Biol Chem.* 2007;282:31257-31266.
- Baron AD, Brechtel G, Wallace P, Edelman SV. Rates and tissue sites of non-insulin-mediated and insulin-mediated glucose-uptake in humans. *Am J Physiol.* 1988;255:E769-E774.
- Bernal-Mizrachi C, Weng S, Li B, et al. Respiratory uncoupling lowers blood pressure through a leptin-dependent mechanism in genetically obese mice. *Arterioscl Throm Vas.* 2002;22:961-968.
- Bernardi P, Rasola A, Forte M, Lippe G. The mitochondrial permeability transition pore: Channel formation by F-ATP synthase, integration in signal transduction, and role in pathophysiology. *Physiol Rev.* 2015;95:1111-1155.
- Biasutto L, Azzolini M, Szabò I, Zoratti M. The mitochondrial permeability transition pore in AD 2016: An update. *BBA-Mol Cell Res.* 2016;1863:2515-2530.
- Brand MD. Mitochondrial generation of superoxide and hydrogen peroxide as the source of mitochondrial redox signaling. *Free Radical Bio Med.* 2016;100:14-31.

- Brand MD, Nicholls DG. Assessing mitochondrial dysfunction in cells. *Biochem J*. 2011;435:297-312.
- Buchanan ID, Nicell JA. Model development for horseradish peroxidase catalyzed removal of aqueous phenol. *Biotechnol Bioeng*. 1997 May;54:251-261.
- Carnagarin R, Dharmarajan AM, Dass CR. Molecular aspects of glucose homeostasis in skeletal muscle—A focus on the molecular mechanisms of insulin resistance. *Mol Cell Endocrinol*. 2015;417:52-62.
- Centers for Disease Control and Prevention. *National Diabetes Statistics Report: Estimates of Diabetes and Its Burden in the United States, 2014*. Atlanta, GA: U.S. Department of Health and Human Services; 2014.
- Cheng AL, Hsu CH, Lin JK, Hsu MM, Ho YF, Shen TS, Ko JY, Lin JT, Lin BR, Ming-Shiang W, Yu HS. Phase I clinical trial of curcumin, a chemopreventive agent, in patients with high-risk or pre-malignant lesions. *Anticancer Res*. 2001;21:2895-2900.
- Chiara F, Castellaro D, Marin O, Petronilli V, Brusilow WS, Juhaszova M, Sollott SJ, Forte M, Bernardi P, Rasola A. Hexokinase II detachment from mitochondria triggers apoptosis through the permeability transition pore independent of voltage-dependent anion channels. *PLoS ONE*. 2008;3:e1852.
- Chuengsamarn S, Rattanamongkolgul S, Luechapudiporn R, Phisalaphong C, Jirawatnotai S. Curcumin extract for prevention of type 2 diabetes. *Diabetes Care*. 2012;35:2121-2127.
- Chuengsamarn S, Rattanamongkolgul S, Phonrat B, Tungtrongchitr R, Jirawatnotai S. Reduction of atherogenic risk in patients with type 2 diabetes by curcuminoid extract: A randomized controlled trial. *J Nutr Biochem*. 2014;25:144-150.
- Clapham JC, Arch JR, Chapman H, Haynes A. Mice overexpressing human uncoupling protein-3 in skeletal muscle are hyperphagic and lean. *Nature*. 2000;406:415-418.
- Clark LC, Sachs G. Bioelectrodes for tissue metabolism. *Ann NY Acad Sci*. 1968;148:133-153.
- Conley KE. Mitochondria to motion: optimizing oxidative phosphorylation to improve exercise performance. *J Exp Biol*. 2016;219:243-249.
- Conley KE, Jubrias SA, Cress ME, Esselman P. Exercise efficiency is reduced by mitochondrial uncoupling in the elderly. *Exp Physiol*. 2013;98:768-77.
- DeFronzo RA, Tripathy D. Skeletal muscle insulin resistance is the primary defect in type 2 diabetes. *Diabetes Care*. 2009 Nov 1;32:S157-S163.

- Deng Y, Chang T, Lee M, Lin J. Suppression of free fatty acid-induced insulin resistance by phytopolyphenols in C2C12 mouse skeletal muscle cells. *J Agric Food Chem*. 2012;60:1059-1066.
- Di Meo S, Iossa S, Venditti P. Skeletal muscle insulin resistance: role of mitochondria and other ROS sources. *J Endocrinol*. 2017;233:R15-R42.
- Divakaruni AS, Brand MD. The regulation and physiology of mitochondrial proton leak. *Physiology*. 2011;26:192-205.
- Dube JJ, Amati F, Toledo FGS, et al. Effects of weight loss and exercise on insulin resistance, and intramyocellular triacylglycerol, diacylglycerol and ceramide. *Diabetologia*. 2011;54:1147-1156.
- Ejaz A, Wu D, Kwan P, Meydani M. Curcumin inhibits adipogenesis in 3T3-L1 adipocytes and angiogenesis and obesity in C57/BL mice. *J Nutr*. 2009;139:919-925.
- El-Moselhy MA, Taye A, Sharkawi SS, El-Sisi SF, Ahmed AF. The antihyperglycemic effect of curcumin in high fat diet fed rats. Role of TNF- α and free fatty acids. *Food Chem Toxicol*. 2011;49:1129-1140.
- Figueiredo VC, Nader GA. Ursolic acid directly promotes protein accretion in myotubes but does not affect myoblast proliferation. *Cell Biochem Funct*. 2012;30:432-437.
- Finck BN, Bernal-Mizrachi C, Han DH, Coleman T, Sambandam N, LaRiviere LL, Holloszy JO, Semenkovich CF, Kelly DP. A potential link between muscle peroxisome proliferator-activated receptor- α signaling and obesity-related diabetes. *Cell Metab*. 2005;1:133-144.
- Fisher-Wellman KH, Neuffer PD. Linking mitochondrial bioenergetics to insulin resistance via redox biology. *Trends Endocrin Met*. 2012;23:142-153.
- Fisher-Wellman KH, Weber TM, Cathey BL, et al. Mitochondrial respiratory capacity and content are normal in young insulin-resistant obese humans. *Diabetes*. 2014;63:132-141.
- Gates AC, Bernal-Mizrachi C, Chinault SL, et al. Respiratory uncoupling in skeletal muscle delays death and diminishes age-related disease. *Cell Metab*. 2007;6:497-505.
- Ghosh S, Banerjee S, Sil PC. The beneficial role of curcumin on inflammation, diabetes and neurodegenerative disease: A recent update. *Food Chem Toxicol*. 2015;83:111-124.
- Gibellini L, Bianchini E, De Biasi S, Nasi M, Cossarizza A, Pinti M. Natural compounds modulating mitochondrial functions. *Evid-Based Compl Alt*. 2015;2015:527209.

Giorgio V, Von Stockum S, Antoniel M, Fabbro A, Fogolari F, Forte M, Glick GD, Petronilli V, Zoratti M, Szabó I, Lippe G. Dimers of mitochondrial ATP synthase form the permeability transition pore. *Proc Natl Acad Sci USA*. 2013;110:5887-5892.

Gnaiger E. Capacity of oxidative phosphorylation in human skeletal muscle: new perspectives of mitochondrial physiology. *Int J Biochem Cell B*. 2009;41:1837-1845.

Gnaiger E. Oxygen conformance of cellular respiration: A perspective of mitochondrial physiology. *Adv Exp Med Biol*. 2003;543:39-55.

Gnaiger E, Lassnig B, Kuznetsov AV, Margreiter R. Mitochondrial respiration in the low oxygen environment of the cell effect of ADP on oxygen kinetics. *BBA-Bioenergetics*. 1998;1365:249-254.

Gnaiger E, Kuznetsov AV. Mitochondrial respiration at low levels of oxygen and cytochrome c. *Biochem Soc T*. 2002;30:252-258.

Gnaiger E, Kuznetsov AV, Rieger G, Amberger A, Fuchs A, Stadlmann S, Eberl T, Margreiter R. Mitochondrial defects by intracellular calcium overload versus endothelial cold ischemia/reperfusion injury. *Transpl Int*. 2000;13:S555-S557.

Gnaiger E, Méndez G, Hand SC. High phosphorylation efficiency and depression of uncoupled respiration in mitochondria under hypoxia. *Proc Natl Acad Sci USA*. 2000;97:11080-11085.

Han D, Nolte L, Ju J, Coleman T, Holloszy J, Semenkovich C. UCP-mediated energy depletion in skeletal muscle increases glucose transport despite lipid accumulation and mitochondrial dysfunction. *Am J Physiol-Endoc M*. 2004;286:E347-E353.

Hardie DG. AMP-activated protein kinase: maintaining energy homeostasis at the cellular and whole-body levels. *Annu Rev Nutr*. 2014;34:31-55.

Hardie DG, Ross FA, Hawley SA. AMP-activated protein kinase: A target for drugs both ancient and modern. *Chem Biol*. 2012;19:1222-1236.

Harper ME, Green K, Brand MD. The efficiency of cellular energy transduction and its implications for obesity. *Annu Rev Nutr*. 2008;28:13-33.

Jang S, Yee S, Choi J, et al. Ursolic acid enhances the cellular immune system and pancreatic beta-cell function in streptozotocin-induced diabetic mice fed a high-fat diet. *Int Immunopharmacol*. 2009;9:113-119.

Jastroch M, Divakaruni AS, Mookerjee S, Treberg JR, Brand MD. Mitochondrial proton and electron leaks. *Essays Biochem*. 2010;47:53-67.

- Jia Y, Kim S, Kim J, et al. Ursolic acid improves lipid and glucose metabolism in high-fat-fed C57BL/6J mice by activating peroxisome proliferator-activated receptor alpha and hepatic autophagy. *Mol Nutr Food Res*. 2015;59:344-354.
- Jiménez-Osorio AS, Monroy A, Alavez S. Curcumin and insulin resistance—Molecular targets and clinical evidences. *Biofactors*. 2016;42:561-580.
- Jonas EA, Porter GA, Beutner G, Mnatsakanyan N, Alavian KN. Cell death disguised: The mitochondrial permeability transition pore as the c-subunit of the F1FO ATP synthase. *Pharmacol Res*. 2015;99:382-392.
- Kang C, Kim E. Synergistic effect of curcumin and insulin on muscle cell glucose metabolism. *Food Chem Toxicol*. 2010;48:2366-2373.
- Katterle Y, Keipert S, Hof J, Klaus S. Dissociation of obesity and insulin resistance in transgenic mice with skeletal muscle expression of uncoupling protein 1. *Physiol Genomics*. 2008;32:352-359.
- Keipert S, Ost M, Chadt A, et al. Skeletal muscle uncoupling-induced longevity in mice is linked to increased substrate metabolism and induction of the endogenous antioxidant defense system. *Am J Physiol-Endoc M*. 2013;304:E495-E506.
- Keipert S, Voigt A, Klaus S. Dietary effects on body composition, glucose metabolism, and longevity are modulated by skeletal muscle mitochondrial uncoupling in mice. *Aging Cell*. 2011;10:122-136.
- Kim JH, Park JM, Kim E, et al. Curcumin stimulates glucose uptake through AMPK-p38 MAPK pathways in L6 myotube cells. *J Cell Physiol*. 2010;223:771-778.
- Klip A, Schertzer JD, Bilan PJ, Thong F, Antonescu C. Regulation of glucose transporter 4 traffic by energy deprivation from mitochondrial compromise. *Acta Physiol*. 2009;196:27-35.
- Korge P, Yang L, Yang JH, Wang Y, Qu Z, Weiss JN. Protective role of transient pore openings in calcium handling by cardiac mitochondria. *J Biol Chem*. 2011;286:34851-34857.
- Krumschnabel G, Fontana-Ayoub M, Sumbalova Z, et al. Simultaneous high-resolution measurement of mitochondrial respiration and hydrogen peroxide production. *Methods Mol Biol*. 2015;1264:245-61.
- Kunkel SD, Elmore CJ, Bongers KS, et al. Ursolic acid increases skeletal muscle and brown fat and decreases diet-induced obesity, glucose intolerance and fatty liver disease. *PLoS ONE*. 2012;7:e39332.

- Kunkel SD, Suneja M, Ebert SM, Bongers KS, Fox DK, Malmberg SE, Alipour F, Shields RK, Adams CM. mRNA expression signatures of human skeletal muscle atrophy identify a natural compound that increases muscle mass. *Cell Metab.* 2011;13:627-638.
- Kunwar A, Barik A, Mishra B, Rathinasamy K, Pandey R, Priyadarsini KI. Quantitative cellular uptake, localization and cytotoxicity of curcumin in normal and tumor cells. *BBA-Gen Subjects.* 2008;1780:673-679.
- Kwak H, Thalacker-Mercer A, Anderson EJ, et al. Simvastatin impairs ADP-stimulated respiration and increases mitochondrial oxidative stress in primary human skeletal myotubes. *Free Radical Bio Med.* 2012;52:198-207.
- Lee HY, Choi CS, Birkenfeld AL, Alves TC, Jornayvaz FR, Jurczak MJ, Zhang D, Woo DK, Shadel GS, Ladiges W, Rabinovitch PS. Targeted expression of catalase to mitochondria prevents age-associated reductions in mitochondrial function and insulin resistance. *Cell Metab.* 2010;12:668-674.
- LeFevre ME. Calibration of Clark oxygen electrode for use in aqueous solutions. *J Appl Physiol.* 1969;26:844-846.
- Lemasters JJ, Theruvath TP, Zhong Z, Nieminen AL. Mitochondrial calcium and the permeability transition in cell death. *BBA-Bioenergetics.* 2009;1787:1395-1401.
- Li B, Nolte L, Ju J, et al. Skeletal muscle respiratory uncoupling prevents diet-induced obesity and insulin resistance in mice. *Nat Med.* 2000;6:1115-1120.
- Li R, Steyn FJ, Stout MB, Lee K, Cully TR, Calderón JC, Ngo ST. Development of a high-throughput method for real-time assessment of cellular metabolism in intact long skeletal muscle fibre bundles. *J Physiol.* 2016;594:7197-7213.
- Li S, Meng F, Liao X, et al. Therapeutic role of ursolic acid on ameliorating hepatic steatosis and improving metabolic disorders in high-fat diet-induced non-alcoholic fatty liver disease rats. *PLoS ONE.* 2014;9:e86724.
- Ligeret H, Barthelemy S, Zini R, Tillement JP, Labidalle S, Morin D. Effects of curcumin and curcumin derivatives on mitochondrial permeability transition pore. *Free Radical Bio Med.* 2004;36:919-929.
- Lim HW, Lim HY, Wong KP. Uncoupling of oxidative phosphorylation by curcumin: Implication of its cellular mechanism of action. *Biochem Bioph Res Co.* 2009;389:187-192.
- Liobikas J, Majiene D, Trumbeckaite S, et al. Uncoupling and antioxidant effects of ursolic acid in isolated rat heart mitochondria. *J Nat Prod.* 2011;74:1640-1644.

- Liu W, Zhai Y, Heng X, Che FY, Chen W, Sun D, Zhai G. Oral bioavailability of curcumin: problems and advancements. *J Drug Target*. 2016;24:694-702.
- Lodi A, Saha A, Lu X, Wang B, Sentandreu E, Collins M, Kolonin MG, DiGiovanni J, Lodi S. Combinatorial treatment with natural compounds in prostate cancer inhibits prostate tumor growth and leads to key modulations of cancer cell metabolism. *NPJ Prec Oncol*. 2017;1:18.
- Long LH, Halliwell B. Artefacts in cell culture: pyruvate as a scavenger of hydrogen peroxide generated by ascorbate or epigallocatechin gallate in cell culture media. *Biochem Bioph Res Co*. 2009;388:700-704.
- Mailloux RJ. Teaching the fundamentals of electron transfer reactions in mitochondria and the production and detection of reactive oxygen species. *Redox Biol*. 2015;4:381-398.
- Makrecka-Kuka M, Krumschnabel G, Gnaiger E. High-resolution respirometry for simultaneous measurement of oxygen and hydrogen peroxide fluxes in permeabilized cells, tissue homogenate and isolated mitochondria. *Biomolecules*. 2015;5:1319-1338.
- Marcinek DJ, Schenkman KA, Ciesielski WA, Conley KE. Mitochondrial coupling in vivo in mouse skeletal muscle. *Am J Physiol-Cell Ph*. 2004;286:C457-C463.
- Marín-Prida J, Andreu GL, Rossignoli CP, Durruthy MG, Rodríguez EO, Reyes YV, Acosta RF, Uyemura SA, Alberici LC. The cytotoxic effects of VE-3N, a novel 1, 4-dihydropyridine derivative, involve the mitochondrial bioenergetic disruption via uncoupling mechanisms. *Toxicol In Vitro*. 2017;42:21-30.
- Martineau LC. Large enhancement of skeletal muscle cell glucose uptake and suppression of hepatocyte glucose-6-phosphatase activity by weak uncouplers of oxidative phosphorylation. *BBA-Gen Subjects*. 2012;1820:133-150.
- Mirzaei H, Shakeri A, Rashidi B, Jalili A, Banikazemi Z, Sahebkar A. Phytosomal curcumin: a review of pharmacokinetic, experimental and clinical studies. *Biomed Pharmacother*. 2017;85:102-112.
- Miyamoto S, Murphy AN, Brown JH. Akt mediates mitochondrial protection in cardiomyocytes through phosphorylation of mitochondrial hexokinase-II. *Cell Death Differ*. 2008;15:521-529.
- Morin D, Barthélémy S, Zini R, Labidalle S, Tillement JP. Curcumin induces the mitochondrial permeability transition pore mediated by membrane protein thiol oxidation. *FEBS Lett*. 2001;495:131-136.
- Muoio DM, Neuffer PD. Lipid-induced mitochondrial stress and insulin action in muscle. *Cell Metab*. 2012;15:595-605.

- Na L, Li Y, Pan H, et al. Curcuminoids exert glucose-lowering effect in type 2 diabetes by decreasing serum free fatty acids: a double-blind, placebo-controlled trial. *Mol Nutr Food Res*. 2013;57:1569-1577.
- Na L, Zhang Y, Li Y, et al. Curcumin improves insulin resistance in skeletal muscle of rats. *Nutr Metab Cardiovas*. 2011;21:526-533.
- Nelson KM, Dahlin JL, Bisson J, Graham J, Pauli GF, Walters MA. The essential medicinal chemistry of curcumin. *J Med Chem*. 2017;60:1620-1637.
- Neschen S, Katterle Y, Richter J, et al. Uncoupling protein 1 expression in murine skeletal muscle increases AMPK activation, glucose turnover, and insulin sensitivity in vivo. *Physiol Genomics*. 2008;33:333-340.
- Ohori K, Miura T, Tanno M, Miki T, Sato T, Ishikawa S, Horio Y, Shimamoto K. Ser9 phosphorylation of mitochondrial GSK-3 β is a primary mechanism of cardiomyocyte protection by erythropoietin against oxidant-induced apoptosis. *Am J Physiol-Heart C*. 2008;295:H2079-H2086.
- Orrenius S, Gogvadze V, Zhivotovsky B. Calcium and mitochondria in the regulation of cell death. *Biochem Biophys Res Commun*. 2015;460:72-81.
- Pastorino JG, Hoek JB, Shulga N. Activation of glycogen synthase kinase 3 β disrupts the binding of hexokinase II to mitochondria by phosphorylating voltage-dependent anion channel and potentiates chemotherapy-induced cytotoxicity. *Cancer Res*. 2005;65:10545-10554.
- Perevoshchikova IV, Quinlan CL, Orr AL, Gerencser AA, Brand MD. Sites of superoxide and hydrogen peroxide production during fatty acid oxidation in rat skeletal muscle mitochondria. *Free Radical Bio Med*. 2013;61:298-309.
- Perry RJ, Kim T, Zhang XM, Lee HY, Pesta D, Popov VB, Zhang D, Rahimi Y, Jurczak MJ, Cline GW, Spiegel DA. Reversal of hypertriglyceridemia, fatty liver disease, and insulin resistance by a liver-targeted mitochondrial uncoupler. *Cell Metab*. 2013;18:740-748.
- Perry RJ, Zhang D, Zhang XM, Boyer JL, Shulman GI. Controlled-release mitochondrial protonophore reverses diabetes and steatohepatitis in rats. *Science*. 2015;347:1253-1256.
- Pesta D, Gnaiger E. High-resolution respirometry: OXPHOS protocols for human cells and permeabilized fibers from small biopsies of human muscle. *Methods Mol Biol*. 2012;810:25-58.
- Petronilli V, Miotto G, Canton M, Brini M, Colonna R, Bernardi P, Di Lisa F. Transient and long-lasting openings of the mitochondrial permeability transition pore can be monitored directly in intact cells by changes in mitochondrial calcein fluorescence. *Biophys J*. 1999;76:725-734.

Plumb JA, Milroy R, Kaye SB. Effects of the pH dependence of 3-(4, 5-dimethylthiazol-2-yl)-2, 5-diphenyltetrazolium bromide-formazan absorption on chemosensitivity determined by a novel tetrazolium-based assay. *Cancer Res.* 1989;49:4435-4440.

Prasad S, Tyagi AK, Aggarwal BB. Recent developments in delivery, bioavailability, absorption and metabolism of curcumin: the golden pigment from golden spice. *Cancer Res Treat.* 2014;46:2-18.

Qiu Y, Yu T, Wang W, Pan K, Shi D, Sun H. Curcumin-induced melanoma cell death is associated with mitochondrial permeability transition pore (mPTP) opening. *Biochem Bioph Res Co.* 2014;448:15-21.

Rasola A, Sciacovelli M, Pantic B, Bernardi P. Signal transduction to the permeability transition pore. *FEBS Lett.* 2010;584:1989-1996.

Ravindran J, Prasad S, Aggarwal BB. Curcumin and cancer cells: How many ways can curry kill tumor cells selectively? *AAPS J.* 2009;11:495-510.

Rindler PM, Crewe CL, Fernandes J, Kinter M, Szweda LI. Redox regulation of insulin sensitivity due to enhanced fatty acid utilization in the mitochondria. *Am J Physiol-Heart C.* 2013;305:H634-H643.

Robey RA, Hay N. Mitochondrial hexokinases, novel mediators of the antiapoptotic effects of growth factors and Akt. *Oncogene.* 2006;25:4683-4696.

Rolfe DF, Newman JM, Buckingham JA, Clark MG, Brand MD. Contribution of mitochondrial proton leak to respiration rate in working skeletal muscle and liver and to SMR. *Am J Physiol-Cell Ph.* 1999;276:C692-C699.

Salabei JK, Gibb AA, Hill BG. Comprehensive measurement of respiratory activity in permeabilized cells using extracellular flux analysis. *Nature Protoc.* 2014;9:421-438.

Salem M, Rohani S, Gillies ER. Curcumin, a promising anti-cancer therapeutic: a review of its chemical properties, bioactivity and approaches to cancer cell delivery. *RSC Adv.* 2014;4:10815-10829.

Scandurra FM, Gnaiger E. Cell respiration under hypoxia: facts and artefacts in mitochondrial oxygen kinetics. *Adv Exp Med Biol.* 2010;662:7-25.

Schafer FQ, Buettner GR. Redox environment of the cell as viewed through the redox state of the glutathione disulfide/glutathione couple. *Free Radical Bio Med.* 2001;30:1191-1212.

Schlagowski AI, Singh F, Charles AL, Ramamoorthy TG, Favret F, Piquard F, Geny B, Zoll J. Mitochondrial uncoupling reduces exercise capacity despite several skeletal muscle metabolic adaptations. *J Appl Physiol.* 2014;116:364-375.

- Sordillo PP, Helson L. Curcumin and cancer stem cells: curcumin has asymmetrical effects on cancer and normal stem cells. *Anticancer Res.* 2015;35:599-614.
- Suresh D, Srinivasan K. Tissue distribution & elimination of capsaicin, piperine & curcumin following oral intake in rats. *Indian J Med Res.* 2010;131:682-691.
- Thrush A, Dent R, McPherson R, Harper ME. Implications of mitochondrial uncoupling in skeletal muscle in the development and treatment of obesity. *FEBS J.* 2013;280:5015-5029.
- Tseng YH, Cypess AM, Kahn CR. Cellular bioenergetics as a target for obesity therapy. *Nat Rev Drug Discov.* 2010;9:465-481.
- Wang K, Fan H, Chen Q, Ma G, Zhu M, Zhang X, Zhang Y, Yu J. Curcumin inhibits aerobic glycolysis and induces mitochondrial-mediated apoptosis through hexokinase II in human colorectal cancer cells in vitro. *Anti-Cancer Drug.* 2015;26:15-24.
- Yaffe D, Saxel OR. Serial passaging and differentiation of myogenic cells isolated from dystrophic mouse muscle. *Nature.* 1977;270:725-727.
- Yang KY, Lin LC, Tseng TY, Wang SC, Tsai TH. Oral bioavailability of curcumin in rat and the herbal analysis from *Curcuma longa* by LC–MS/MS. *J Chromatogr B.* 2007;853:183-189.
- Zheng J, Ramirez VD. Inhibition of mitochondrial proton F₀F₁-ATPase/ATP synthase by polyphenolic phytochemicals. *Brit J Pharmacol.* 2000;130:1115-1123.